Electronic Supplementary Information

Molecular Recognition and Spectral Tuning of Organic Dyes in Water by Amide Naphthotubes

Zhao Chen,[a,b] Mao Quan,[b] Yi-Wei Dong,[b] Ming-Shuang Li,[b] Song-Meng Wang,[b] Lei-Min Zhao,[b] Liu-Pan Yang, *[b,c] Jishan Wu*[a] and Wei Jiang,*[b]

[a.] *Department of Chemistry, National University of Singapore, 3 Science Drive 3, 117543, Singapore. E-mail: chmwuj@nus.edu.sg.*
[b.] *Shenzhen Grubbs Institute, Guangdong Provincial Key Laboratory of Catalysis and Department of Chemistry, Southern University of Science and Technology, Xueyuan Blvd 1088, Shenzhen, 518055, China. E-mail: jiangw@sustech.edu.cn.*
[c.] *School of Pharmaceutical Science, Hengyang Medical School, University of South China, Hengyang, 421001, China. E-mail: yanglp@usc.edu.cn.*

Table of Contents

1. General Methods

Experimental Method. All the reagents and guest molecules involved in this research were commercially available and used without further purification unless otherwise noted. Solvents were either employed as purchased or dried prior to use by standard laboratory procedures. ^{1}H NMR spectra were recorded on a Bruker Avance-400 or 500 NMR spectrometer. All chemical shifts are reported in ppm with residual solvents as the internal standards. Fluorescence spectra were obtained on a Shimadzu RF-5301pc spectrometer. UV−vis absorption spectra were obtained on a Hitachi U-2600 UV−vis spectrophotometer. Emission lifetime measurements were performed with Hamamatsu compact fluorescence lifetime spectrometer C11367. Absolute luminescent quantum yields were recorded with Hamamatsu absolute PL quantum yield spectrometer C11347. Circular dichroism (CD) spectra were recorded on an Applied PhotoPhysics Chirascan CD spectropolarimeter, using a 1 cm quartz cuvette. The synthetic procedure of **1a** and **1b** has been reported in our previous work. [1,2]

ITC Titrations. Isothermal Titration Calorimetry (ITC) experiments were carried out in deionized water at 25 °C on a VP-ITC instrument (Malvern MicroCal VP-ITC) and a Malvern MicroCal PEAQ-ITC Automated instrument for three times. The ± values in the ITC means the standard errors of the mean in three times titration. Errors are smaller than ±10%.

UV-vis titrations. For UV-vis titrations, a solution of the corresponding dye (the concentration is 2.5×10^{-5} M unless otherwise noted) prepared in phosphate buffer (pH =7.4). This solution was placed in a cuvette (2.0 mL) at 25 °C. The sample was then titrated with a solution of a host. Nonlinear curve-fitting method was then used to obtain the association constants through the following equation:

$$Int=I_0+(((Igh-I_0)/2)/H_0)*(H_0+G_0+1/K_a-sqrt((H_0+G_0+1/K_a)\text{^}2-4*H_0*G_0))$$

Fluorescence titrations. For fluorescence titrations, a 1.0×10^{-5} M solution of the corresponding dye prepared in phosphate buffer (pH =7.4). This solution was placed in a cuvette (2.0 mL) at 25 °C. The sample was then titrated with a solution of a host.

2. ^{1}H NMR Spectra of Host-Guest Complexes

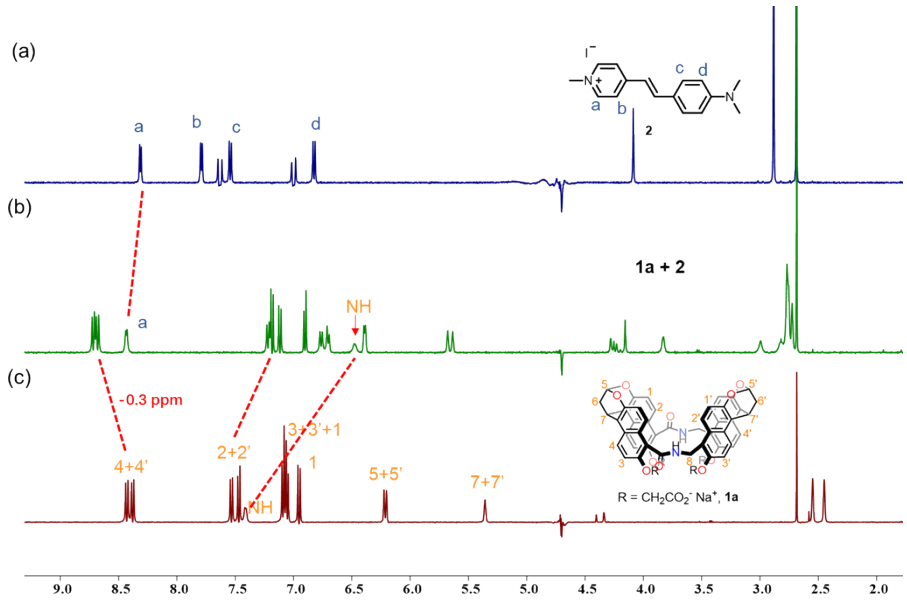

Fig. S1. ^{1}H NMR spectra (500 MHz, 0.5 mM, H_2O/D_2O = 9:1, 298 K) of (a) **2**, (c) **1a**, and (b) their equimolar mixture in PB buffer (50 mM). In the 1:1 mixture, the aromatic protons of the host shift upfield or downfield, and NH proton shift upfield, supporting the binding between **1a** and **2**. The guest exchange is fast at the NMR time scale and some NMR signals of the guest became broadened or disappeared into the baseline.

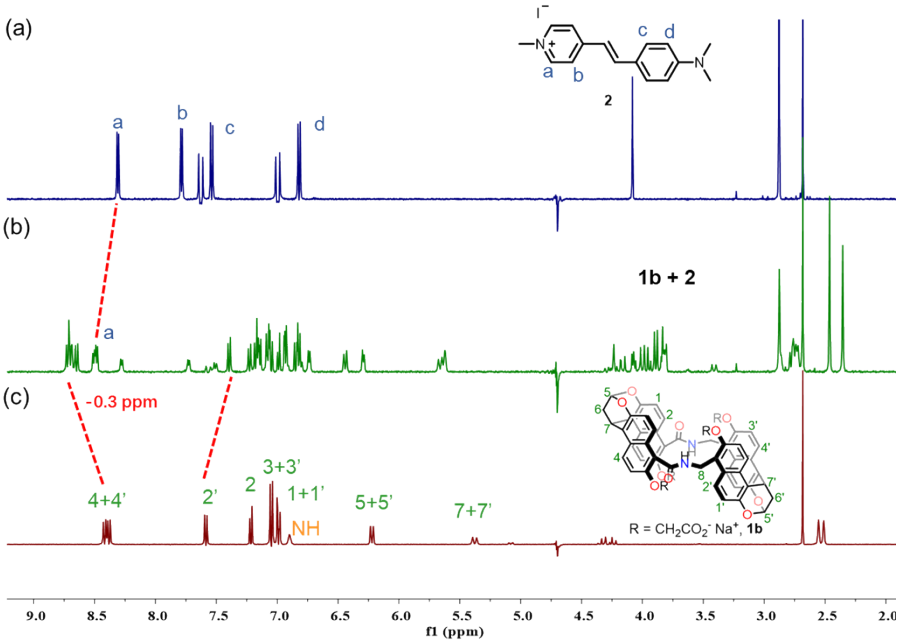

Fig. S2. ^{1}H NMR spectra (500 MHz, 0.5 mM, H_2O/D_2O = 9:1, 298 K) of (a) **2**, (c) **1b**, and (b) their equimolar mixture in PB buffer (pH 7.4). In the 1:1 mixture, the protons

of the host shift obviously, supporting the binding between **1b** and **2**. The splitting of the protons of the host indicates the binding is slow exchange at the NMR time scale and the host become de-symmetrised after binding the guest **2**.

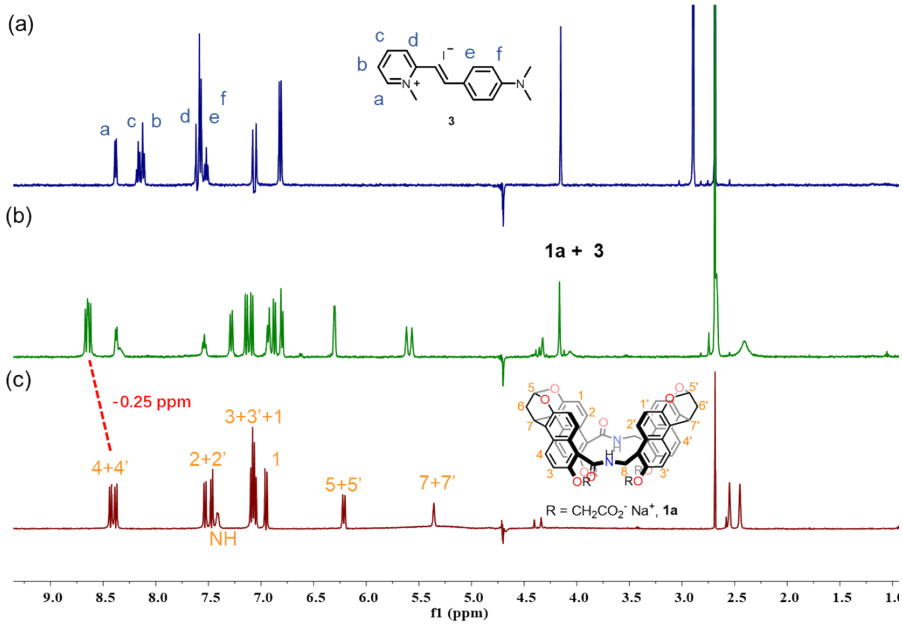

Fig. S3. ^{1}H NMR spectra (500 MHz, 0.5 mM, H_2O/D_2O = 9:1, 298 K) of (a) **3**, (c) **1a**, and (b) their equimolar mixture in PB buffer (pH 7.4). In the 1:1 mixture, the aromatic protons of the host and guest underwent obvious shift, supporting the binding between **1a** and **3**.

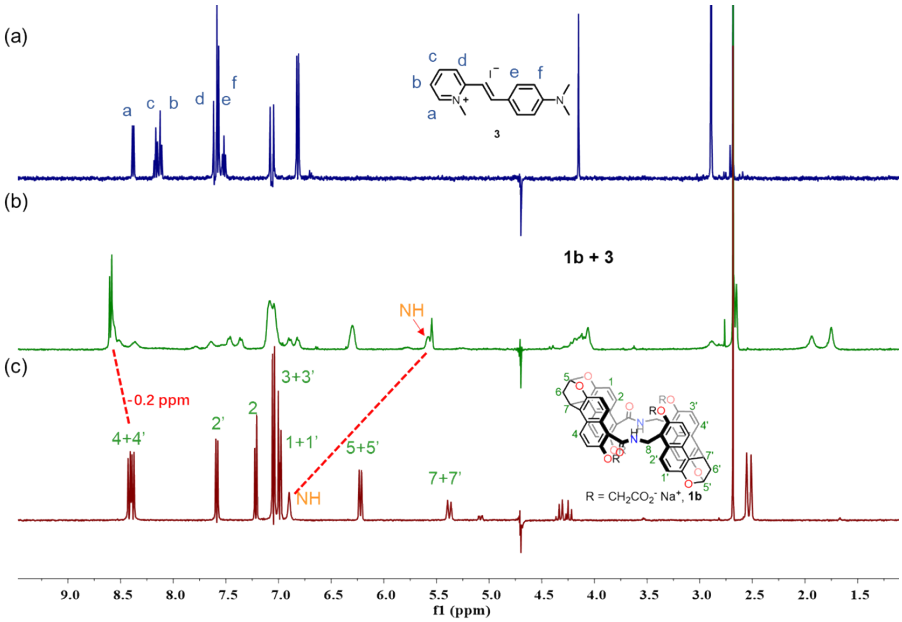

Fig. S4. ^{1}H NMR spectra (500 MHz, 0.5 mM, H_2O/D_2O = 9:1, 298 K) of (a) **3**, (c) **1b**, and (b) their equimolar mixture in PB buffer (pH 7.4). In the 1:1 mixture, the peaks are broadened and underwent obvious shift, supporting the binding between **1b** and **3**.

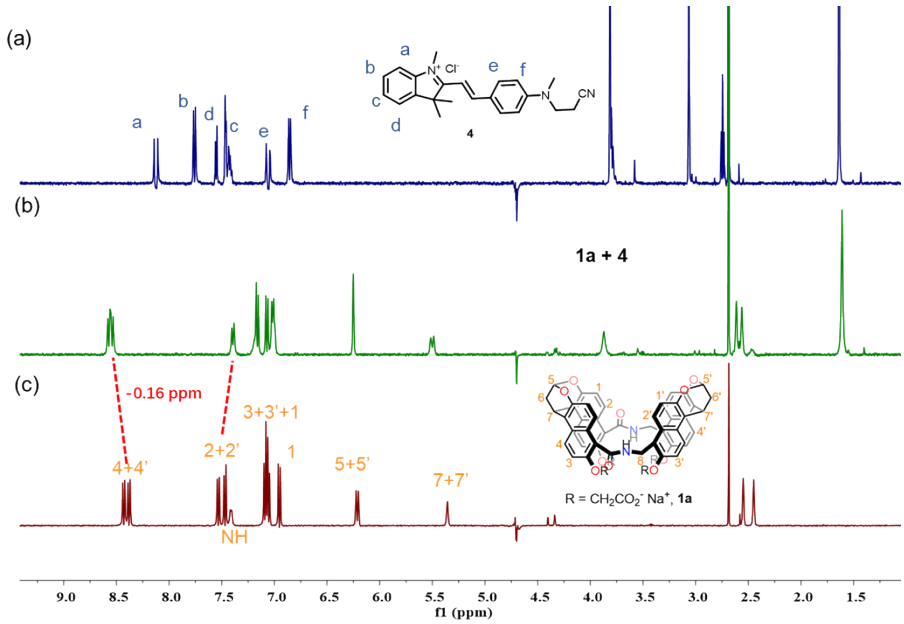

Fig. S5. ^{1}H NMR spectra (500 MHz, 0.5 mM, H_2O/D_2O = 9:1, 298 K) of (a) **4**, (c) **1a**, and (b) their equimolar mixture in PB buffer (pH 7.4). In the 1:1mixture, the aromatic protons of the host went obvious shift, while the aromatic protons of the guest became broadened and disappeared into baseline, supporting the binding between **1a** and **4**.

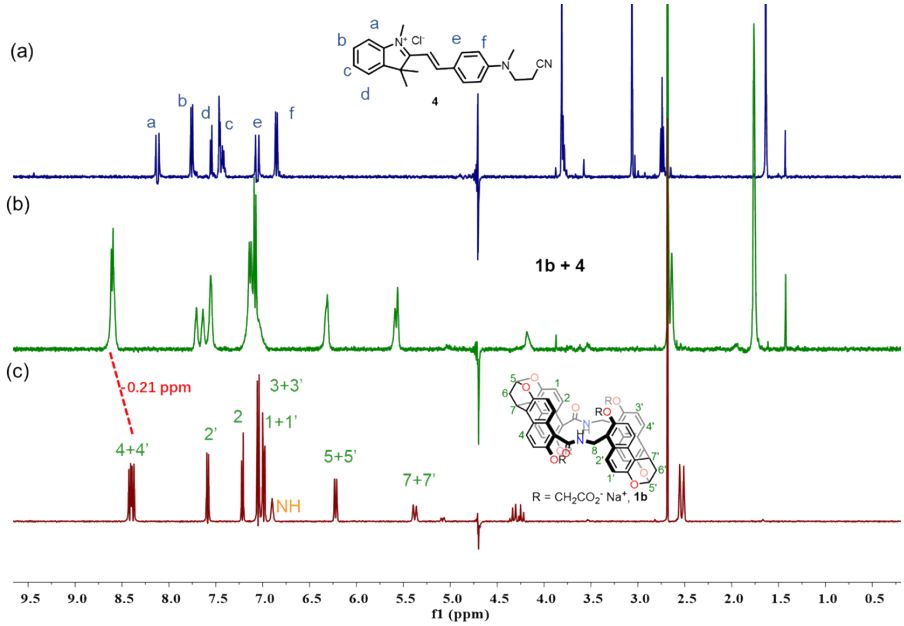

Fig. S6. ^{1}H NMR spectra (500 MHz, 0.5 mM, H_2O/D_2O = 9:1, 298 K) of (a) **4**, (c) **1b**, and (b) their equimolar mixture in PB buffer (pH 7.4). In the 1:1 mixture, the peaks of the host underwent obvious shift, while the peaks of the guest became broad and disappeared into the baseline, supporting the binding between **1b** and **4**.

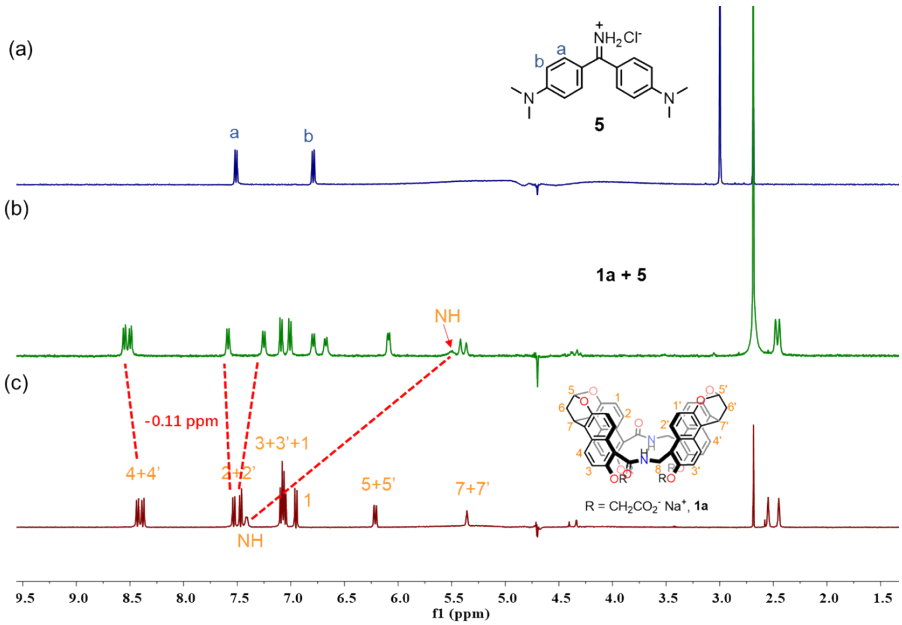

Fig. S7. ^{1}H NMR spectra (500 MHz, 0.5 mM, H_2O/D_2O = 9:1, 298 K) of (a) **5**, (c) **1a**, and (b) their equimolar mixture in PB buffer (pH 7.4). In the 1:1 mixture, the aromatic protons of the host and NH proton underwent obvious shift, and the peaks of the guest became broad and disappeared into baseline, supporting a binding event occurs.

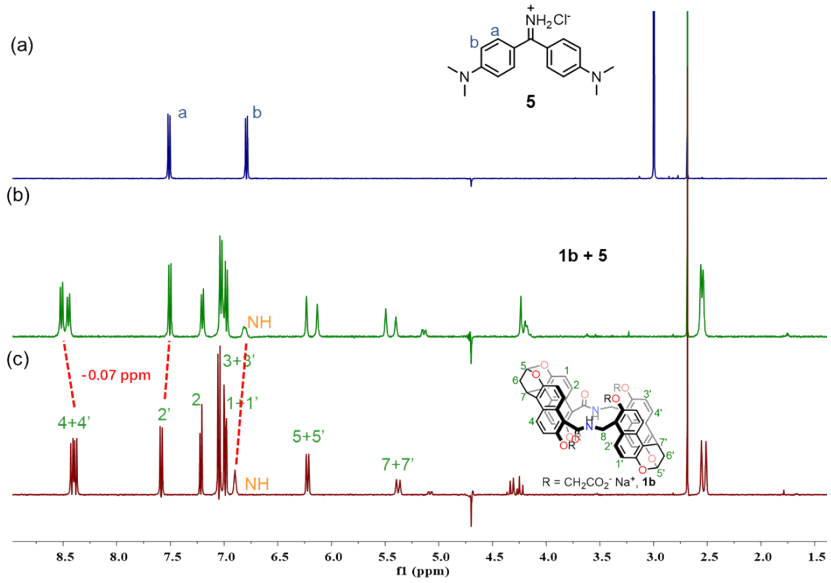

Fig. S8. ^{1}H NMR spectra (500 MHz, 0.5 mM, H_2O/D_2O = 9:1, 298 K) of (a) **5**, (c) **1b**, and (b) their equimolar mixture in PB buffer (pH 7.4). In the 1:1 mixture, the aromatic protons of the host and NH proton experiences obvious shift, while the aromatic protons of the guest became broad and disappeared into the baseline, supporting the binding between **1b** and **5**.

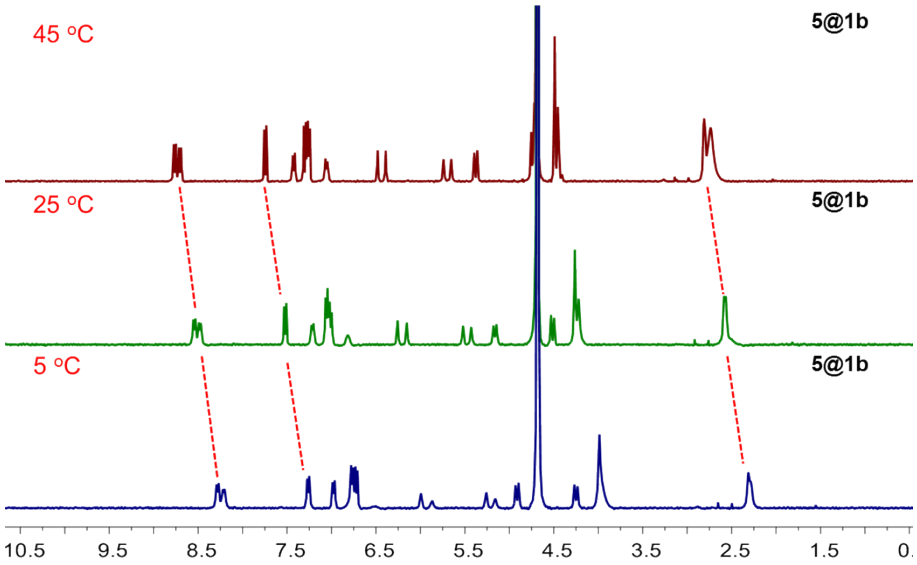

Fig. S9. ^{1}H NMR spectra (400 MHz, 2.0 mM, D_2O) of 1:1 mixture of **5** with **1b** at different temperature. The signals of the complex shift upfield as the temperature drops. However, at the three temperatures, the guest signals are all disappeared into baseline and cann't be observed.

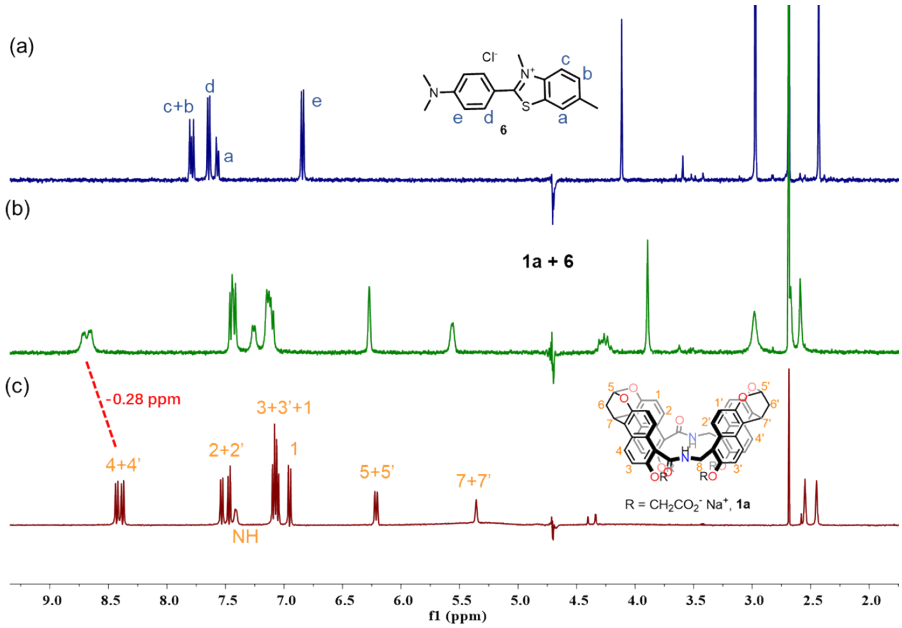

Fig. S10. ^{1}H NMR spectra (500 MHz, 0.5 mM, H_2O/D_2O = 9:1, 298 K) of (a) **6**, (c) **1a**, and (b) their equimolar mixture in PB buffer (pH 7.4). In the 1:1 mixture, the peaks of the host are broadened and underwent obvious shift, while the aromatic protons of the guest became broad and disappeared into the baseline, supporting the binding between **1a** and **6**.

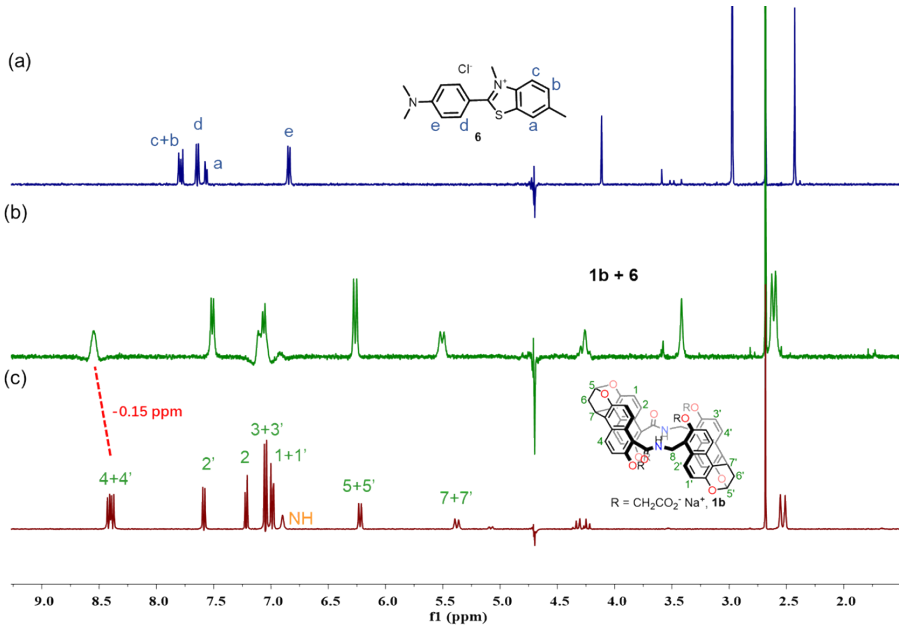

Fig. S11. ^{1}H NMR spectra (500 MHz, 0.5 mM, H_2O/D_2O = 9:1, 298 K) of (a) **6**, (c) **1b**, and (b) their equimolar mixture in PB buffer (pH 7.4). In the 1:1 mixture, the peaks of the host became broadened and underwent obvious shift, while the aromatic protons of the guest became broad and disappeared into the baseline, supporting the binding between **1b** and **6**.

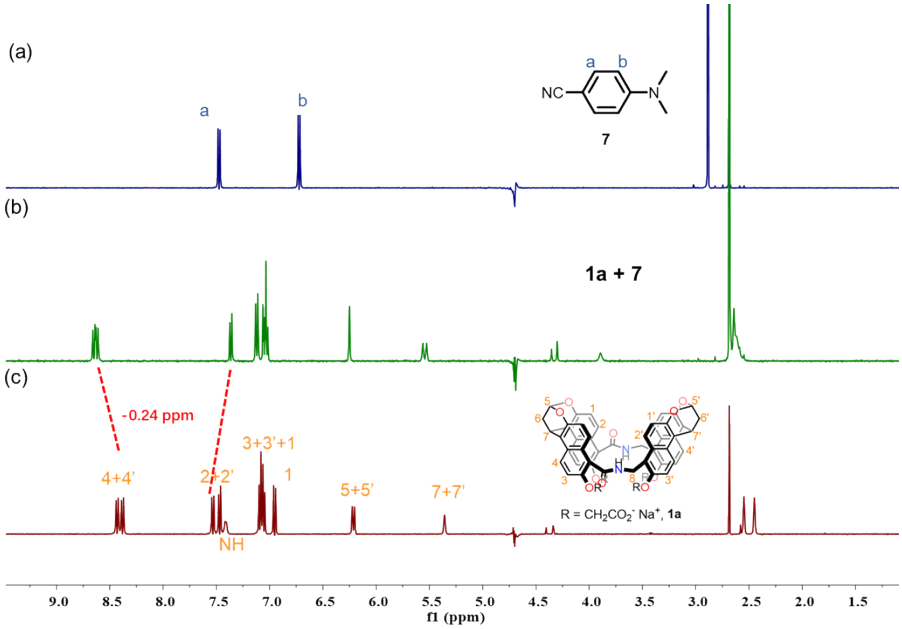

Fig. S12. ^{1}H NMR spectra (500 MHz, 0.5 mM, H_2O/D_2O = 9:1, 298 K) of (a) **7**, (c) **1a**, and (b) their equimolar mixture in PB buffer (pH 7.4). In the 1:1 mixture, the aromatic protons of the host underwent obvious shift, while the aromatic protons of the guest became broad and disappeared into the baseline, supporting the binding between **1a** and **7**.

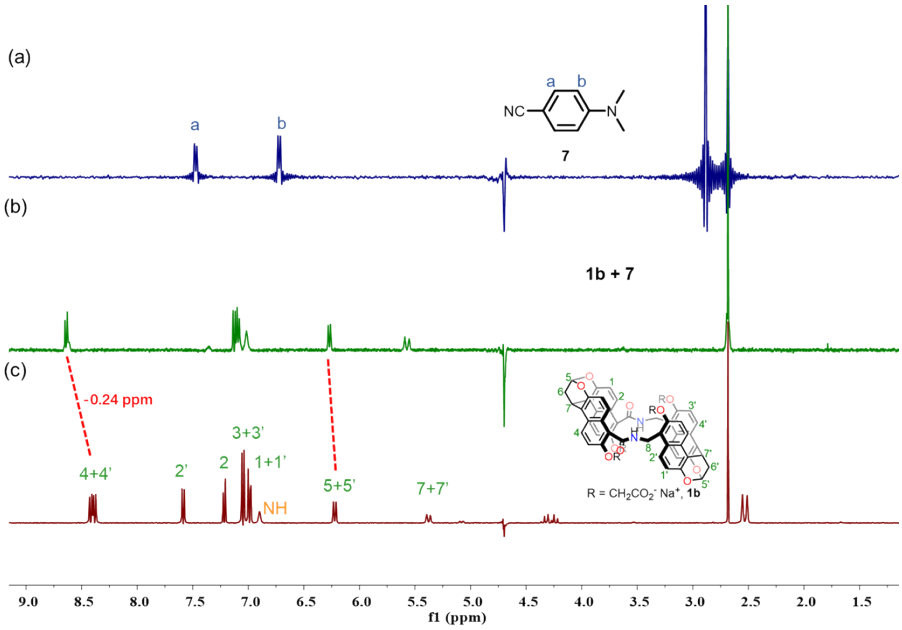

Fig. S13. ^{1}H NMR spectra (500 MHz, 0.5 mM, H_2O/D_2O = 9:1, 298 K) of (a) **7**, (c) **1b**, and (b) their equimolar mixture in PB buffer (pH 7.4). In the spectrum of their mixture, the peaks of the host under obvious shift, while the aromatic protons of the guest became broad and disappeared into the baseline, supporting the binding between **1b** and **7**.

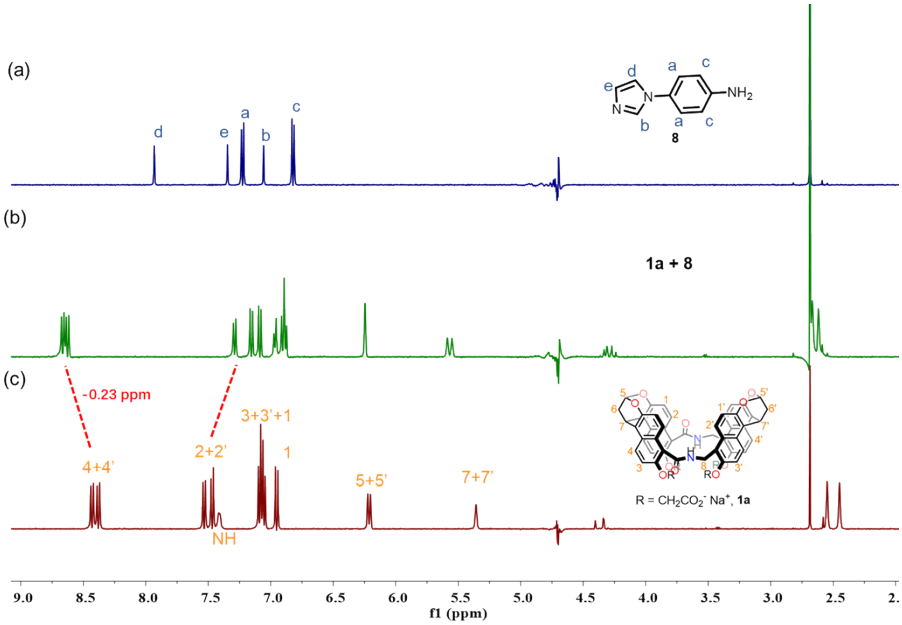

Fig. S14. ^{1}H NMR spectra (500 MHz, 0.5 mM, H_2O/D_2O = 9:1, 298 K) of (a) **8**, (c) **1a**, and (b) their equimolar mixture in PB buffer (pH 7.4). In the 1:1 mixture, the aromatic protons of the host underwent obvious shift, while the aromatic protons of the guest became broad and disappeared into the baseline, supporting the binding between **1a** and **8**.

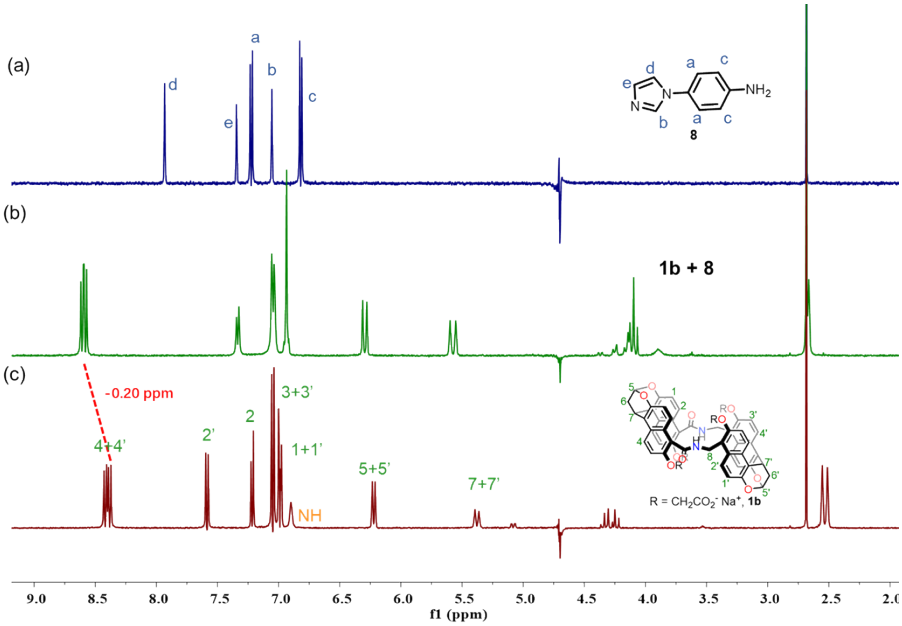

Fig. S15. ^{1}H NMR spectra (500 MHz, 0.5 mM, H_2O/D_2O = 9:1, 298 K) of (a) **8**, (c) **1b**, and (b) their equimolar mixture in PB buffer (pH 7.4). In the 1:1 mixture, the aromatic protons of the host experiences obvious shift, while the aromatic protons of the guest became broadened and disappeared into the baseline, supporting the binding between **1b** and **8**.

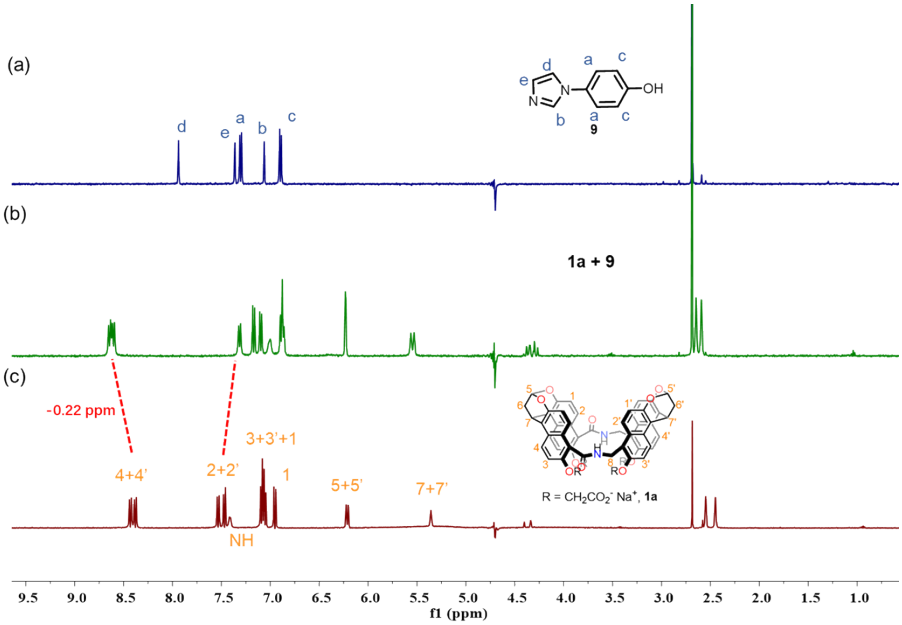

Fig. S16. ^{1}H NMR spectra (500 MHz, 0.5 mM, H_2O/D_2O = 9:1, 298 K) of (a) **9**, (c) **1a**, and (b) their equimolar mixture in PB buffer (pH 7.4). In the 1:1 mixture, the peaks of the hos shift obviously, while the aromatic protons of the guest became broad and disappeared into the baseline, supporting the binding between **1a** and **9**.

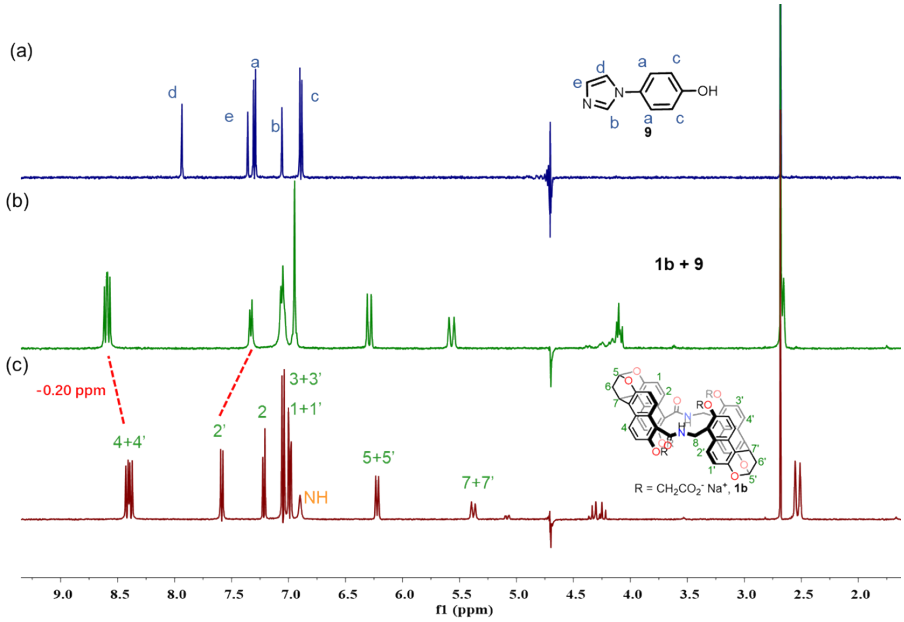

Fig. S17. ^{1}H NMR spectra (500 MHz, 0.5 mM, H_2O/D_2O = 9:1, 298 K) of (a) **9**, (c) **1b**, and (b) their equimolar mixture in PB buffer (pH 7.4). In the 1:1 mixture, the peaks of the host shifted obviously, while the aromatic protons of the guest became broad and disappeared into the baseline, supporting the binding between **1b** and **9**.

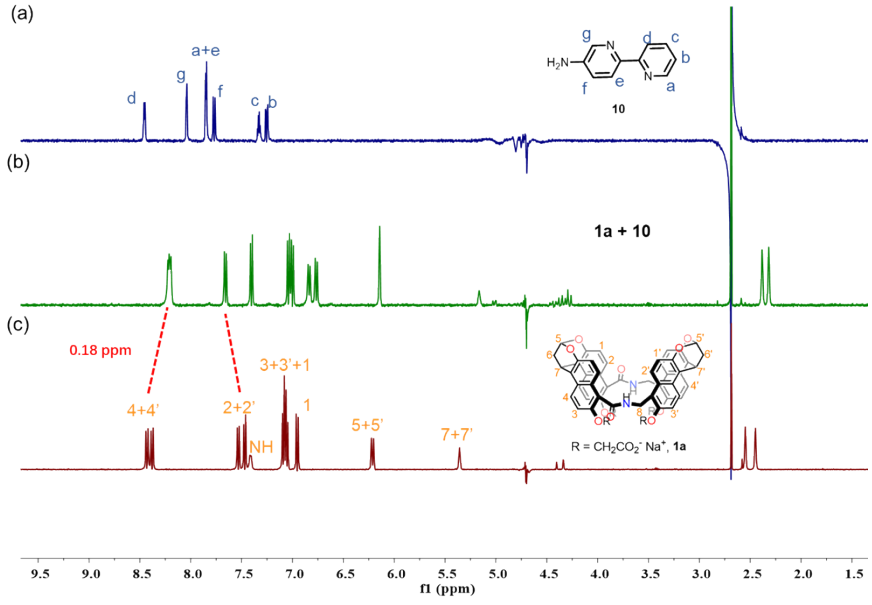

Fig. S18. ^{1}H NMR spectra (500 MHz, 0.2 mM, H_2O/D_2O = 9:1, 298 K) of (a) **10**, (c) **1a**, and (b) their equimolar mixture in PB buffer (pH 7.4). In the 1:1 mixture, the peaks of the host went shifted obviously, while the aromatic protons of the guest became broad and disappeared into baseline, supporting a binding event occurs.

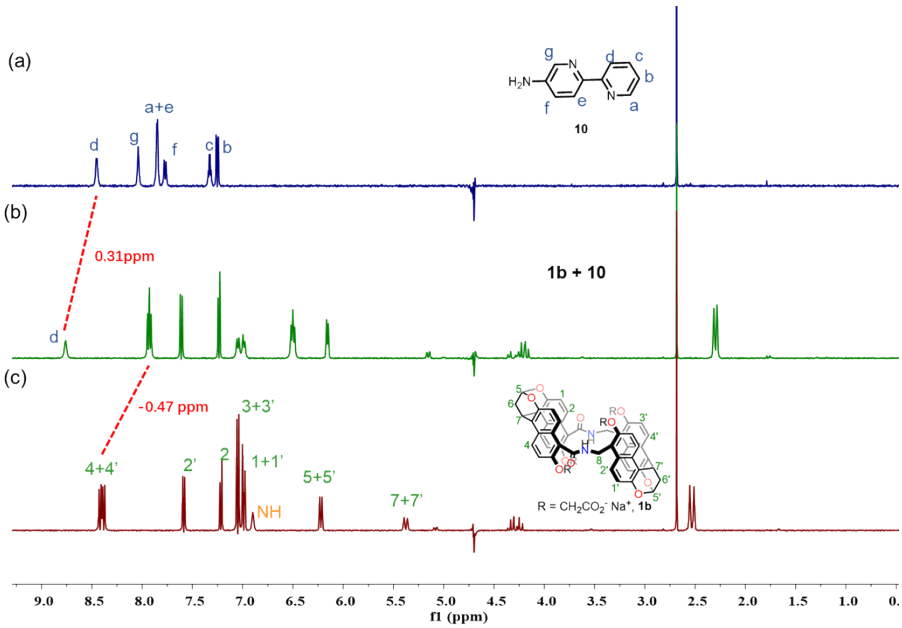

Fig. S19. ^{1}H NMR spectra (500 MHz, 0.2 mM, H_2O/D_2O = 9:1, 298 K) of (a) **10**, (c) **1b**, and (b) their equimolar mixture in PB buffer (pH 7.4). In the 1:1 mixture, the peaks of the host and guest shifted obviously, supporting the binding between **1b** and **10**.

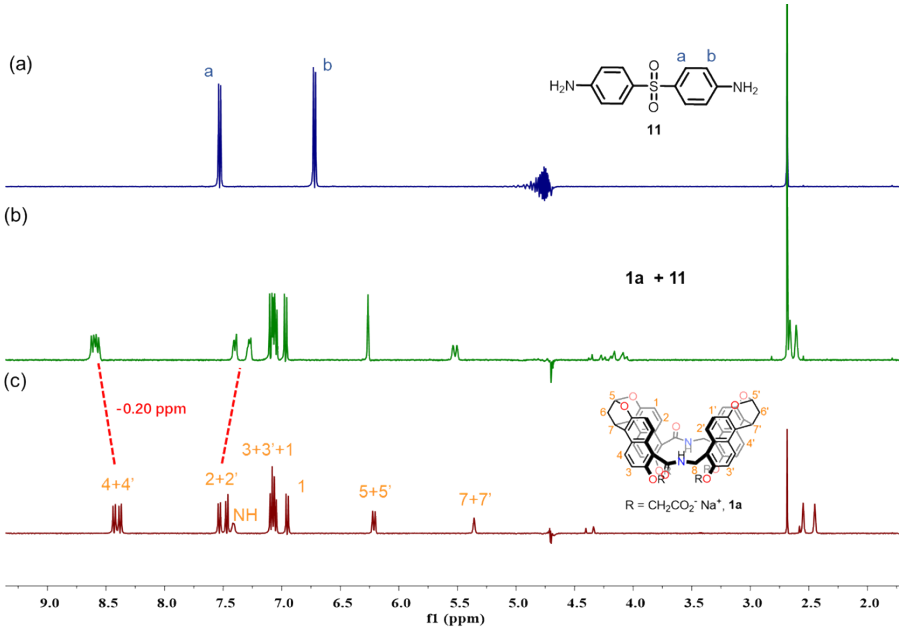

Fig. S20. ^{1}H NMR spectra (500 MHz, 0.2 mM, H_2O/D_2O = 9:1, 298 K) of (a) **11**, (c) **1a**, and (b) their equimolar mixture in PB buffer (pH 7.4). In the 1:1 mixture, the peaks of the host shifted obviously, while the aromatic protons of the guest became broadened and disappeared into the baseline, supporting the binding between **1a** and **11**.

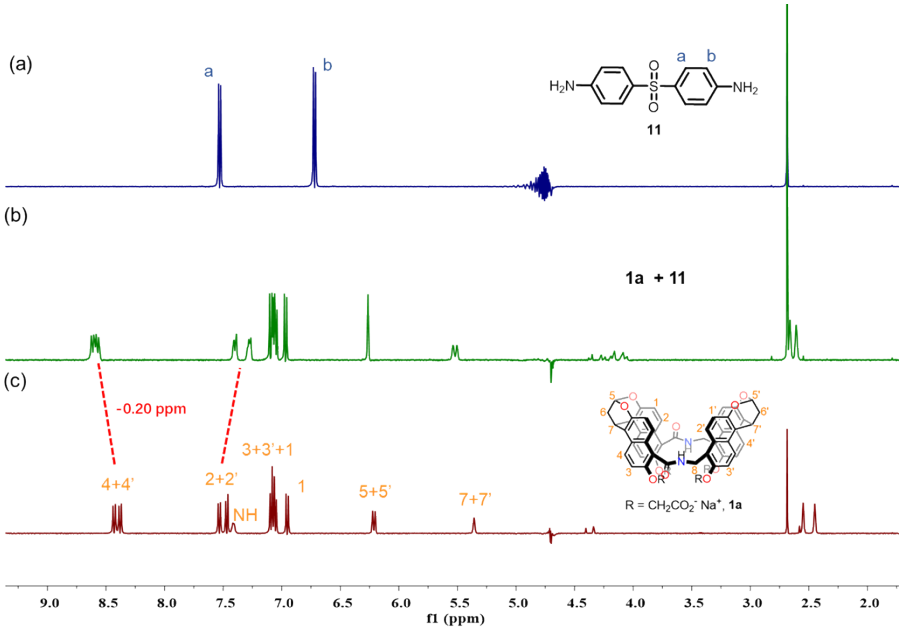

Fig. S21. ^{1}H NMR spectra (500 MHz, 0.2 mM, H_2O/D_2O = 9:1, 298 K) of (a) **11**, (c) **1b**, and (b) their equimolar mixture in PB buffer (pH 7.4). In the 1:1 mixture, the peaks of the host shifted obviously, while the aromatic protons of the guest disappeared into the baseline, supporting the binding between **1b** and **11**.

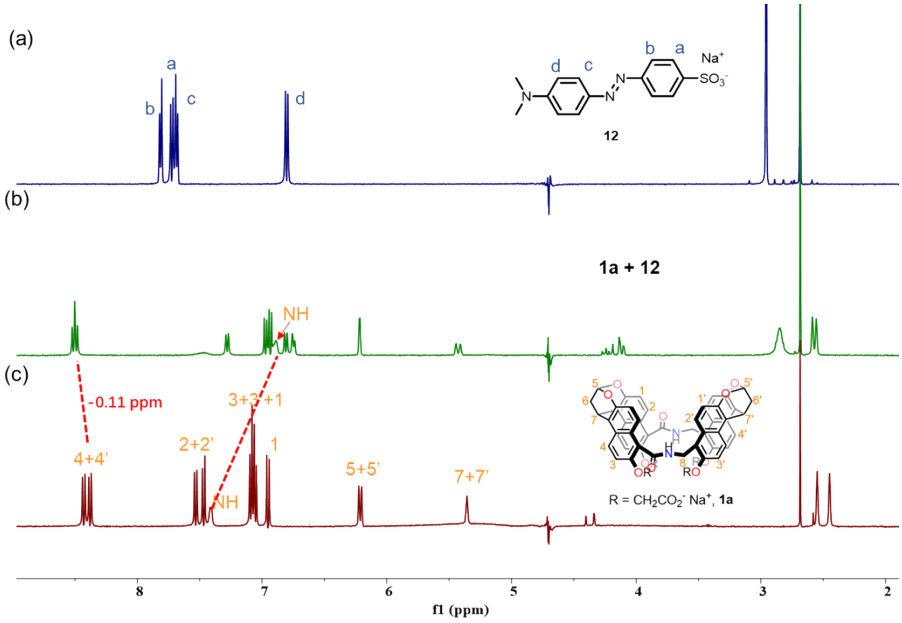

Fig. S22. ^{1}H NMR spectra (500 MHz, 0.5 mM, H_2O/D_2O = 9:1, 298 K) of (a) **12**, (c) **1a**, and (b) their equimolar mixture in PB buffer (pH 7.4). In the 1:1 mixture, the aromatic protons of the host and NH proton shifted obviously, while the aromatic protons of the guest became broadened or disappeared into the baseline, supporting the binding between **1a** and **12**.

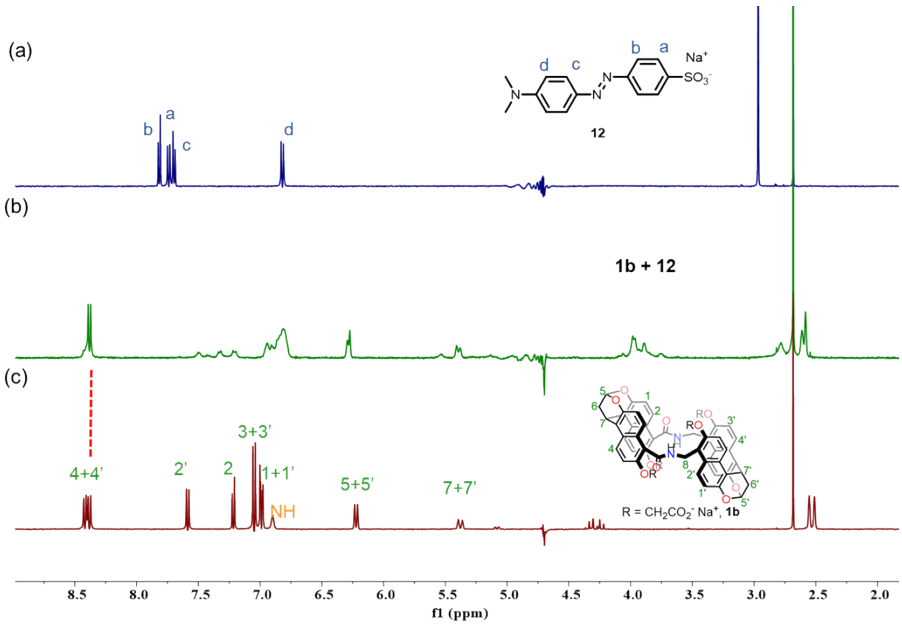

Fig. S23. ^{1}H NMR spectra (500 MHz, 0.5 mM, H_2O/D_2O = 9:1, 298 K) of (a) **12**, (c) **1b**, and (b) their equimolar mixture in PB buffer (pH 7.4). In the 1:1 mixture, the obvious changes of peaks pattern and chemical shifts supporting the binding between **1b** and **12**.

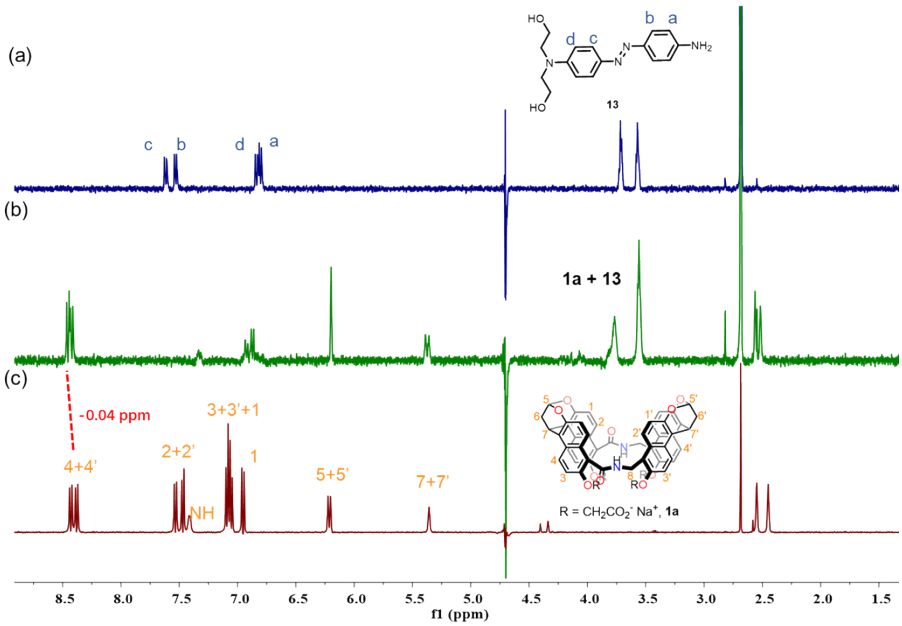

Fig. S24. ^{1}H NMR spectra (500 MHz, 0.5 mM, H_2O/D_2O = 9:1, 298 K) of (a) **13**, (c) **1a**, and (b) their equimolar mixture in PB buffer (pH 7.4). In the 1:1 mixture, the obvious changes of peaks pattern and chemical shifts supporting the binding between **1a** and **13**.

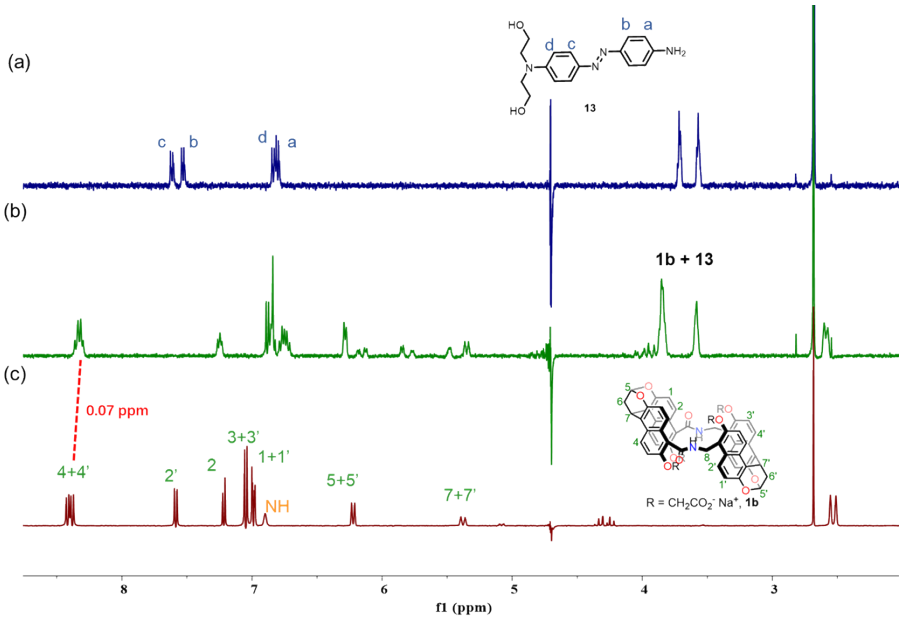

Fig. S25. ^{1}H NMR spectra (500 MHz, 0.5 mM, H_2O/D_2O = 9:1, 298 K) of (a) **13**, (c) **1b**, and (b) their equimolar mixture in PB buffer (pH 7.4). In the 1:1 mixture, the obvious changes of peaks pattern and chemical shifts supporting the binding between **1b** and **13**.

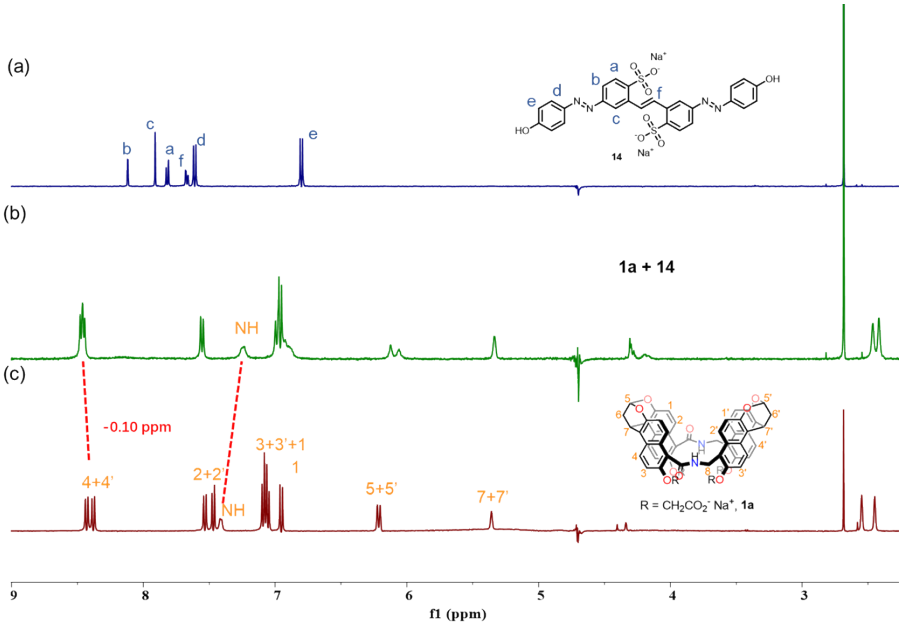

Fig. S26. ^{1}H NMR spectra (500 MHz, 0.5 mM, H_2O/D_2O = 9:1, 298 K) of (a) **14**, (c) **1a**, and (b) their equimolar mixture in PB buffer (pH 7.4). In the 1:1 mixture, the obvious changes of peaks pattern and chemical shifts supporting the binding between **1a** and **14**.

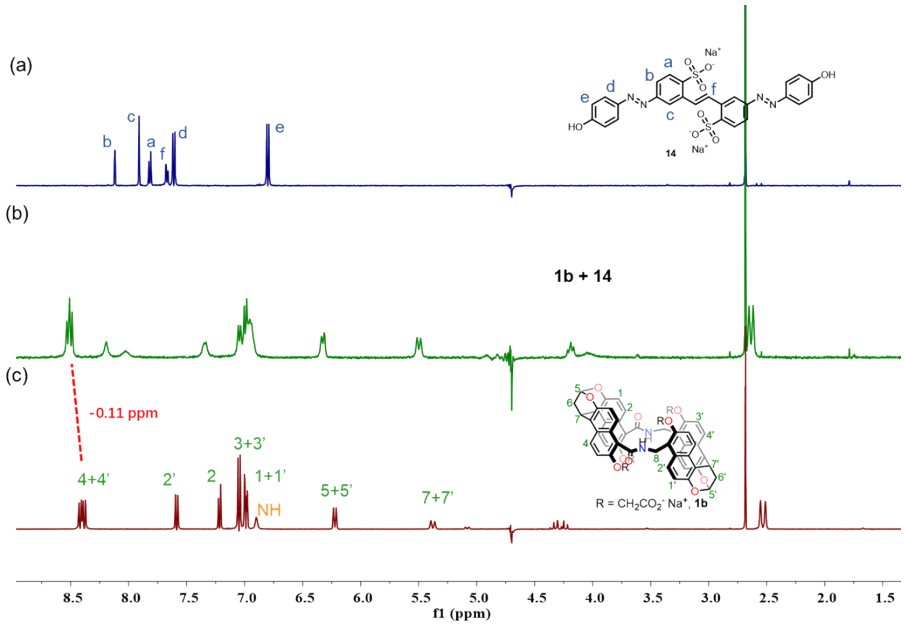

Fig. S27. ^{1}H NMR spectra (500 MHz, 0.5 mM, H_2O/D_2O = 9:1, 298 K) of (a) **14**, (c) **1b**, and (b) their equimolar mixture in PB buffer (pH 7.4). In the 1:1 mixture, the obvious changes of peaks pattern and chemical shifts supporting the binding between **1b** and **14**. The NH proton became broad or disappeared.

3. Binding Constants of 1a and 1b by ITC titration

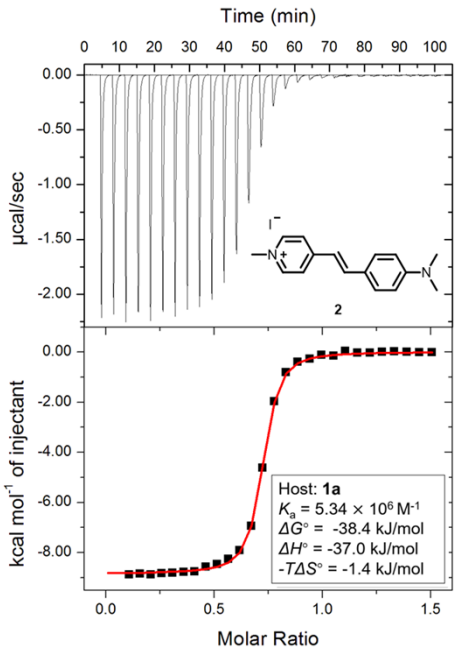

	K_a (M^{-1})	$\Delta G°$ (kJ/mol)
1st	5.77 × 10^6	-38.6
2nd	4.96 × 10^6	-38.2
3rd	5.34 × 10^6	-38.4
average	(5.36 ± 0.33) × 10^6	-38.4 ± 0.2

	$\Delta H°$ (kJ/mol)	$-T\Delta S°$ (kJ/mol)
1st	-38.1	-0.5
2nd	-38.4	0.2
3rd	-37.0	-1.4
average	-37.8 ± 0.6	-0.6 ± 0.6

Fig. S28. ITC titration plots (heat rate versus time and heat versus guest/host ratio) of **2** to **1a** in phosphate buffer (pH =7.4) at 298 K. In this titration, the concentration of host is 0.1 mM, the concentration of guest is 0.5 mM.

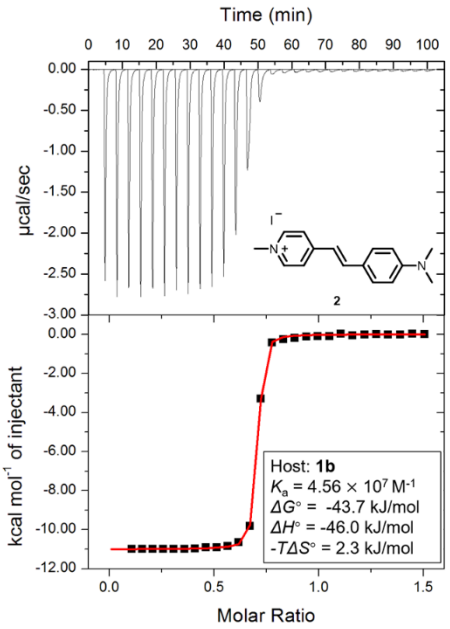

	K_a (M^{-1})	$\Delta G°$ (kJ/mol)
1st	4.31 × 10^7	-43.6
2nd	4.56 × 10^7	-43.7
3rd	4.70 × 10^7	-43.9
average	(4.52 ± 0.16) × 10^7	-43.7 ± 0.1

	$\Delta H°$ (kJ/mol)	$-T\Delta S°$ (kJ/mol)
1st	-46.1	2.5
2nd	-46.0	2.3
3rd	-46.1	2.2
average	-46.1 ± 0.1	2.3 ± 0.1

Fig. S29. ITC titration plots (heat rate versus time and heat versus guest/host ratio) of **2** to **1b** in phosphate buffer (pH =7.4) at 298 K. In this titration, the concentration of host is 0.1 mM, the concentration of guest is 0.7 mM.

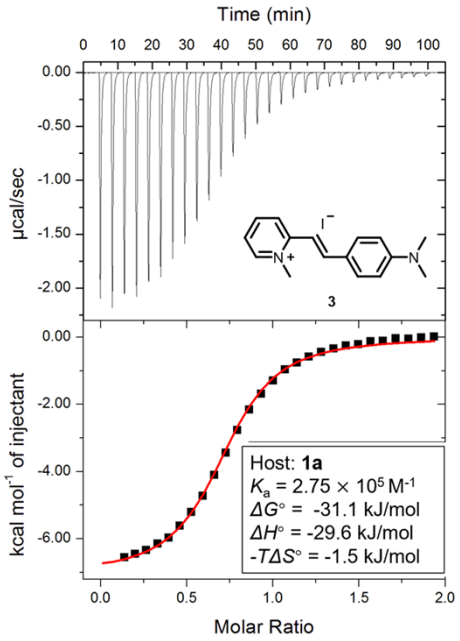

	K_a (M^{-1})	$\Delta G°$ (kJ/mol)
1st	2.67×10^5	-31.0
2nd	2.75×10^5	-31.1
3rd	2.90×10^5	-31.2
average	$(2.77 \pm 0.10) \times 10^5$	-31.1 ± 0.1

	$\Delta H°$ (kJ/mol)	$-T\Delta S°$ (kJ/mol)
1st	-30.0	-1.0
2nd	-29.6	-1.5
3rd	-28.5	-2.7
average	-29.4 ± 0.6	-1.7 ± 0.7

Fig. S30. ITC titration plots (heat rate versus time and heat versus guest/host ratio) of **3** to **1a** in phosphate buffer (pH =7.4) at 298 K. In this titration, the concentration of host is 0.1 mM, the concentration of guest is 0.9 mM.

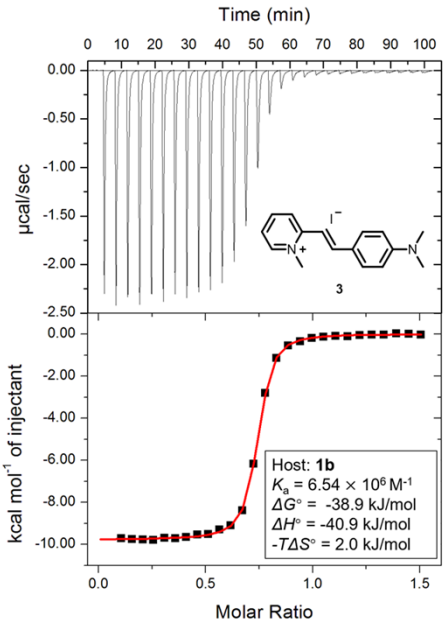

	K_a (M^{-1})	$\Delta G°$ (kJ/mol)
1st	6.19×10^6	-38.8
2nd	6.54×10^6	-38.9
3rd	6.21×10^6	-38.8
average	$(6.31 \pm 0.16) \times 10^6$	-38.8 ± 0.1

	$\Delta H°$ (kJ/mol)	$-T\Delta S°$ (kJ/mol)
1st	-41.2	2.4
2nd	-40.9	2.0
3rd	-41.1	2.3
average	-41.1 ± 0.1	2.2 ± 0.2

Fig. S31. ITC titration plots (heat rate versus time and heat versus guest/host ratio) of **3** to **1b** in phosphate buffer (pH =7.4) at 298 K. In this titration, the concentration of host is 0.1 mM, the concentration of guest is 0.7 mM.

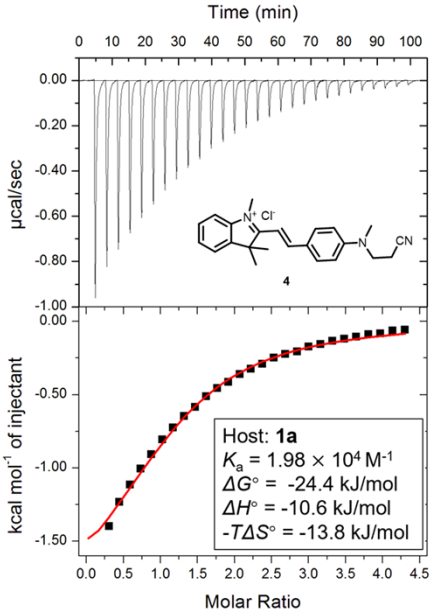

	K_a (M^{-1})	$\Delta G°$ (kJ/mol)
1st	1.98×10^4	-24.4
2nd	1.90×10^4	-24.4
3rd	1.75×10^4	-24.3
average	$(1.88 \pm 0.10) \times 10^4$	-24.4 ± 0.1

	$\Delta H°$ (kJ/mol)	$-T\Delta S°$ (kJ/mol)
1st	-10.6	-13.8
2nd	-9.1	-15.3
3rd	-9.1	-15.2
average	-9.6 ± 0.7	-14.8 ± 0.7

Fig. S32. ITC titration plots (heat rate versus time and heat versus guest/host ratio) of **4** to **1a** in phosphate buffer (pH =7.4) at 298 K. In this titration, the concentration of host is 0.1 mM, the concentration of guest is 2.0 mM.

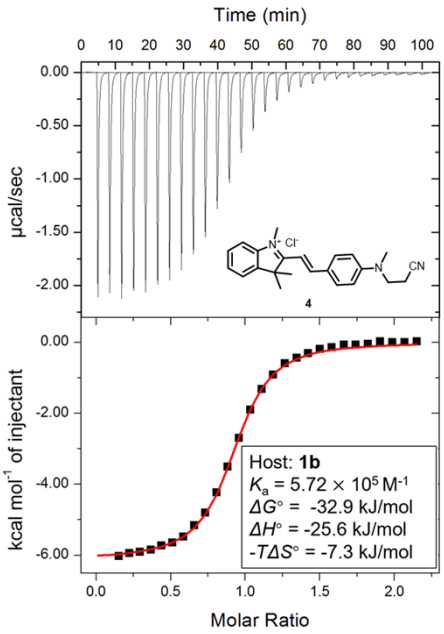

	K_a (M^{-1})	$\Delta G°$ (kJ/mol)
1st	5.67×10^5	-32.9
2nd	5.51×10^5	-32.7
3rd	5.72×10^5	-32.9
average	$(5.63 \pm 0.09) \times 10^5$	-32.8 ± 0.1

	$\Delta H°$ (kJ/mol)	$-T\Delta S°$ (kJ/mol)
1st	-26.0	-6.9
2nd	-26.0	-6.7
3rd	-25.6	-7.3
average	-25.9 ± 0.2	-7.0 ± 0.2

Fig. S33. ITC titration plots (heat rate versus time and heat versus guest/host ratio) of **4** to **1b** in phosphate buffer (pH =7.4) at 298 K. In this titration, the concentration of host is 0.1 mM, the concentration of guest is 1.0 mM.

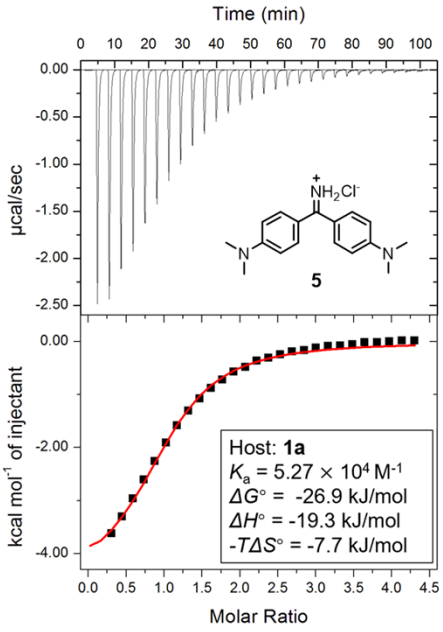

	K_a (M^{-1})	$\Delta G°$ (kJ/mol)
1st	4.99×10^4	-26.9
2nd	5.04×10^4	-26.9
3rd	5.27×10^4	-26.9
average	$(5.10 \pm 0.12) \times 10^4$	-26.9 ± 0.1

	$\Delta H°$ (kJ/mol)	$-T\Delta S°$ (kJ/mol)
1st	-21.4	-5.4
2nd	-21.3	-5.5
3rd	-19.3	-7.7
average	-20.6 ± 1.0	-6.2 ± 1.1

Fig. S34. ITC titration plots (heat rate versus time and heat versus guest/host ratio) of **5** to **1a** in phosphate buffer (pH =7.4) at 298 K. In this titration, the concentration of host is 0.1 mM, the concentration of guest is 2.0 mM

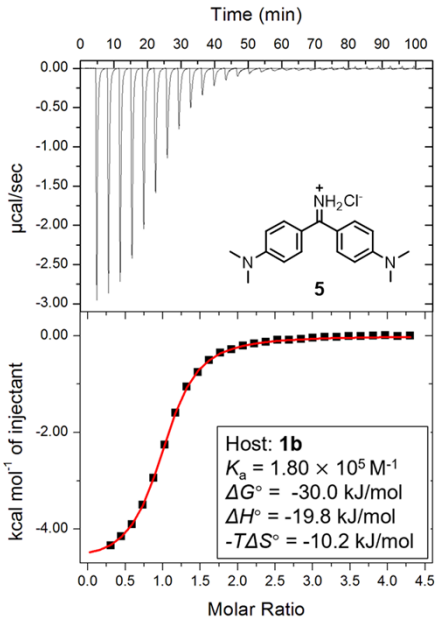

	K_a (M^{-1})	$\Delta G°$ (kJ/mol)
1st	1.64×10^5	-29.8
2nd	1.80×10^5	-30.0
3rd	1.75×10^5	-29.9
average	$(1.73 \pm 0.07) \times 10^5$	-29.9 ± 0.1

	$\Delta H°$ (kJ/mol)	$-T\Delta S°$ (kJ/mol)
1st	-19.9	-9.9
2nd	-19.8	-10.2
3rd	-19.2	-10.7
average	-19.6 ± 0.3	-10.2 ± 0.3

Fig. S35. ITC titration plots (heat rate versus time and heat versus guest/host ratio) of **5** to **1b** in phosphate buffer (pH =7.4) at 298 K. In this titration, the concentration of host is 0.1 mM, the concentration of guest is 2.0 mM.

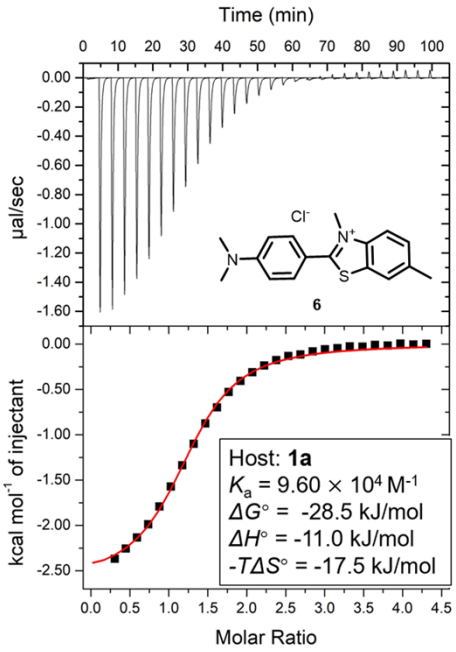

	K_a (M^{-1})	$\Delta G°$ (kJ/mol)
1st	9.19×10^4	-28.2
2nd	9.60×10^4	-28.5
3rd	9.40×10^4	-28.4
average	$(9.40 \pm 0.17) \times 10^4$	-28.4 ± 0.1

	$\Delta H°$ (kJ/mol)	$-T\Delta S°$ (kJ/mol)
1st	-10.9	-17.3
2nd	-11.0	-17.5
3rd	-11.1	-17.3
average	-11.0 ± 0.1	-17.4 ± 0.1

Fig. S36. ITC titration plots (heat rate versus time and heat versus guest/host ratio) of **6** to **1a** in phosphate buffer (pH =7.4) at 298 K. In this titration, the concentration of host is 0.1 mM, the concentration of guest is 2.0 mM.

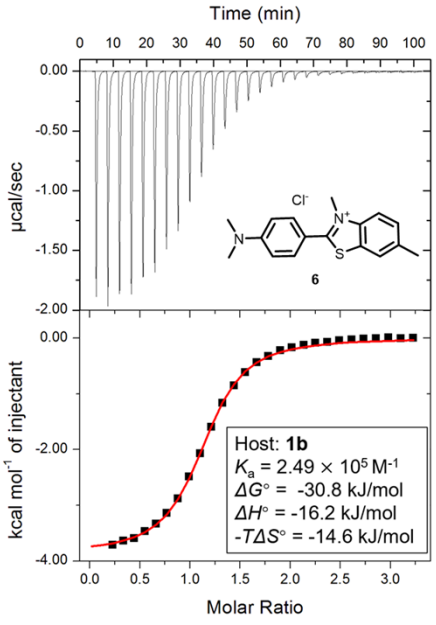

	K_a (M^{-1})	$\Delta G°$ (kJ/mol)
1st	2.18×10^5	-30.4
2nd	2.49×10^5	-30.8
3rd	2.61×10^5	-31.0
average	$(2.43 \pm 0.18) \times 10^5$	-30.7 ± 0.2

	$\Delta H°$ (kJ/mol)	$-T\Delta S°$ (kJ/mol)
1st	-16.1	-14.3
2nd	-16.2	-14.6
3rd	-15.9	-15.1
average	-16.1 ± 0.1	-14.7 ± 0.3

Fig. S37. ITC titration plots (heat rate versus time and heat versus guest/host ratio) of **6** to **1b** in phosphate buffer (pH =7.4) at 298 K. In this titration, the concentration of host is 0.1 mM, the concentration of guest is 1.5 mM.

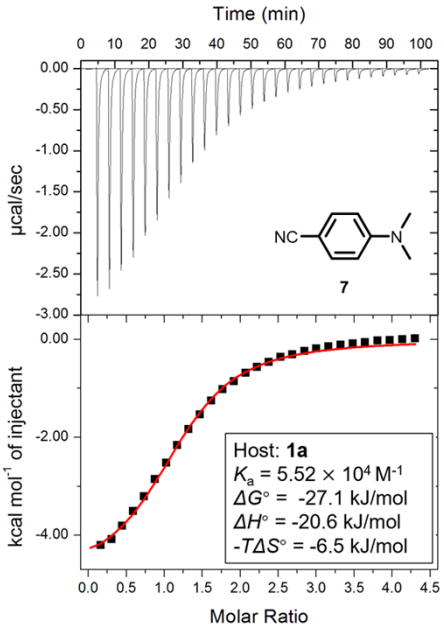

	K_a (M^{-1})	$\Delta G°$ (kJ/mol)
1st	5.46×10^4	-27.0
2nd	5.57×10^4	-27.1
3rd	5.52×10^4	-27.1
average	$(5.52 \pm 0.04) \times 10^4$	-27.1 ± 0.1

	$\Delta H°$ (kJ/mol)	$-T\Delta S°$ (kJ/mol)
1st	-20.6	-6.4
2nd	-20.4	-6.7
3rd	-20.6	-6.5
average	-20.5 ± 0.1	-6.5 ± 0.1

Fig. S38. ITC titration plots (heat rate versus time and heat versus guest/host ratio) of **7** to **1a** in phosphate buffer (pH =7.4) at 298 K. In this titration, the concentration of host is 2.0 mM, the concentration of guest is 0.1 mM.

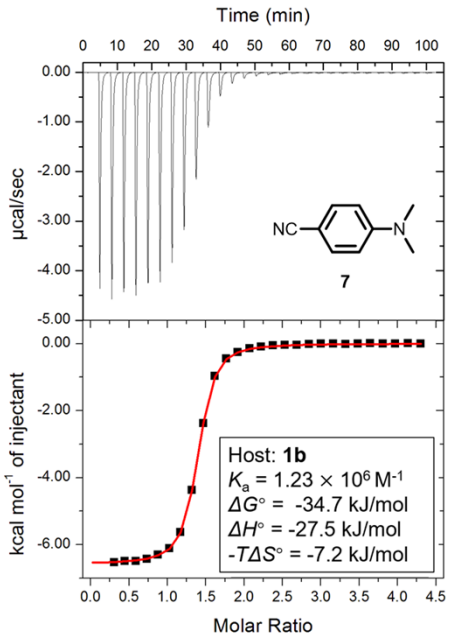

	K_a (M^{-1})	$\Delta G°$ (kJ/mol)
1st	1.23×10^6	-34.7
2nd	1.22×10^6	-34.7
3rd	1.23×10^6	-34.7
average	$(1.23 \pm 0.01) \times 10^6$	-34.7 ± 0.0

	$\Delta H°$ (kJ/mol)	$-T\Delta S°$ (kJ/mol)
1st	-27.5	-7.2
2nd	-27.4	-7.3
3rd	-27.5	-7.2
average	-27.5 ± 0.1	-7.2 ± 0.1

Fig. S39. ITC titration plots (heat rate versus time and heat versus guest/host ratio) of **7** to **1b** in phosphate buffer (pH =7.4) at 298 K. In this titration, the concentration of host is 2.0 mM, the concentration of guest is 0.1 mM.

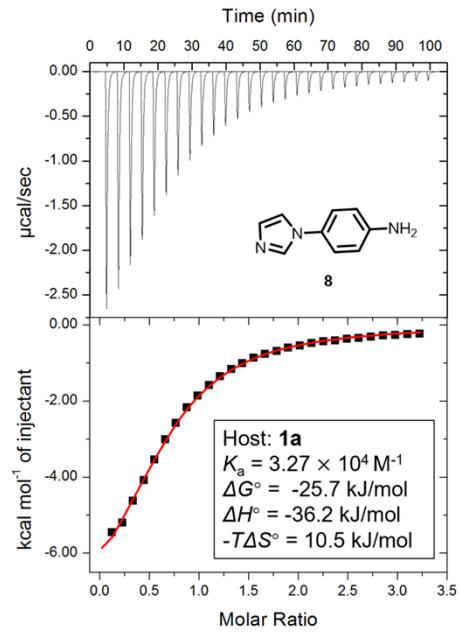

	K_a (M^{-1})	$\Delta G°$ (kJ/mol)
1st	3.27×10^4	-25.8
2nd	3.08×10^4	-25.7
3rd	3.13×10^4	-25.6
average	$(3.16 \pm 0.08) \times 10^4$	-25.7 ± 0.1

	$\Delta H°$ (kJ/mol)	$-T\Delta S°$ (kJ/mol)
1st	-36.2	10.4
2nd	-38.0	12.3
3rd	-39.2	13.6
average	-37.8 ± 1.2	12.1 ± 1.3

Fig. S40. ITC titration plots (heat rate versus time and heat versus guest/host ratio) of **8** to **1a** in phosphate buffer (pH =7.4) at 298 K. In this titration, the concentration of host is 0.1 mM, the concentration of guest is 1.5 mM.

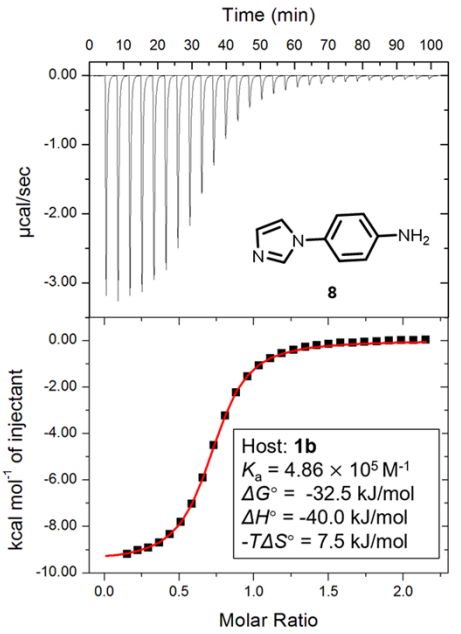

	K_a (M^{-1})	$\Delta G°$ (kJ/mol)
1st	4.86×10^5	-32.5
2nd	4.81×10^5	-32.5
3rd	5.06×10^5	-32.6
average	$(4.91 \pm 0.11) \times 10^5$	-32.5 ± 0.1

	$\Delta H°$ (kJ/mol)	$-T\Delta S°$ (kJ/mol)
1st	-40.0	7.5
2nd	-39.6	7.1
3rd	-39.2	6.6
average	-39.6 ± 0.3	7.1 ± 0.3

Fig. S41. ITC titration plots (heat rate versus time and heat versus guest/host ratio) of **8** to **1b** in phosphate buffer (pH =7.4) at 298 K. In this titration, the concentration of host is 0.1 mM, the concentration of guest is 1.0 mM.

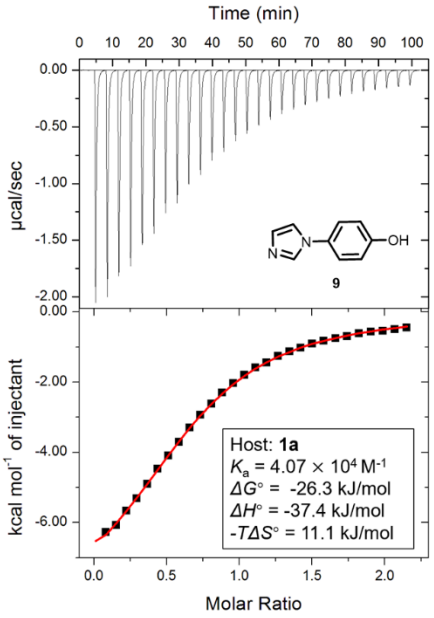

	K_a (M^{-1})	$\Delta G°$ (kJ/mol)
1st	4.07×10^4	-26.3
2nd	3.61×10^4	-26.0
3rd	4.00×10^4	-26.3
average	$(3.89 \pm 0.20) \times 10^4$	-26.2 ± 0.1

	$\Delta H°$ (kJ/mol)	$-T\Delta S°$ (kJ/mol)
1st	-37.4	11.0
2nd	-36.5	10.4
3rd	-34.8	8.5
average	-36.2 ± 1.0	10.0 ± 1.1

Fig. S42. ITC titration plots (heat rate versus time and heat versus guest/host ratio) of **9** to **1a** in phosphate buffer (pH =7.4) at 298 K. In this titration, the concentration of host is 0.1 mM, the concentration of guest is 1.0 mM.

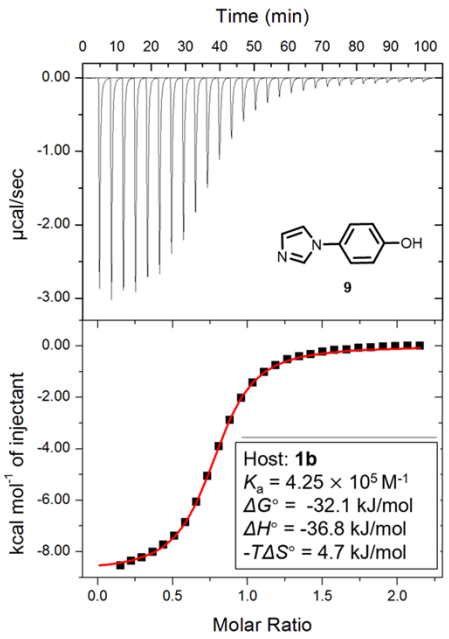

	K_a (M^{-1})	$\Delta G°$ (kJ/mol)
1st	4.47×10^5	-32.3
2nd	4.25×10^5	-32.1
3rd	4.31×10^5	-32.1
average	$(4.34 \pm 0.09) \times 10^5$	-32.2 ± 0.1

	$\Delta H°$ (kJ/mol)	$-T\Delta S°$ (kJ/mol)
1st	-36.4	4.1
2nd	-36.8	4.7
3rd	-36.7	4.6
average	-36.6 ± 0.2	4.4 ± 0.3

Fig. S43. ITC titration plots (heat rate versus time and heat versus guest/host ratio) of **9** to **1b** in phosphate buffer (pH =7.4) at 298 K. In this titration, the concentration of host is 0.1 mM, the concentration of guest is 1.0 mM.

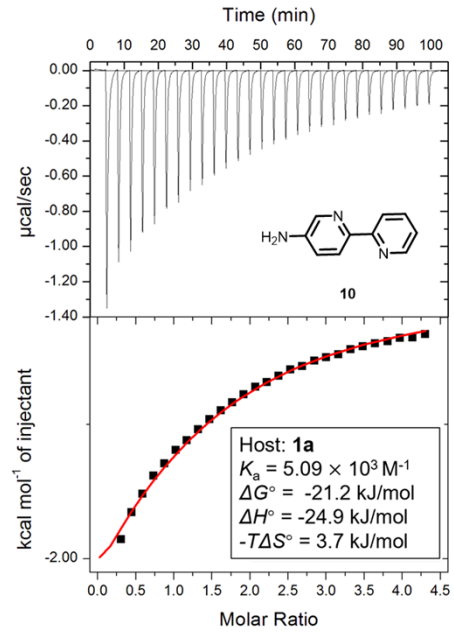

	K_a (M^{-1})	$\Delta G°$ (kJ/mol)
1st	5.20×10^3	-21.2
2nd	5.04×10^3	-21.2
3rd	5.09×10^3	-21.2
average	$(5.11 \pm 0.07) \times 10^3$	-21.2 ± 0.0

	$\Delta H°$ (kJ/mol)	$-T\Delta S°$ (kJ/mol)
1st	-24.4	3.2
2nd	-27.2	6.0
3rd	-24.9	3.7
average	-25.5 ± 1.2	4.3 ± 1.2

Fig. S44. ITC titration plots (heat rate versus time and heat versus guest/host ratio) of **10** to **1a** in phosphate buffer (pH =7.4) at 298 K. In this titration, the concentration of host is 0.1 mM, the concentration of guest is 2.0 mM.

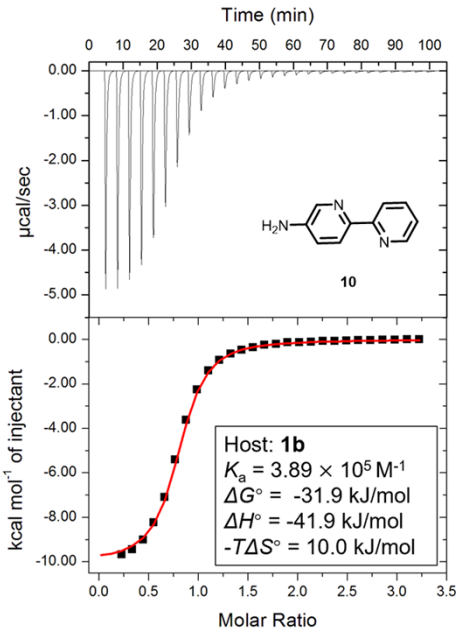

	K_a (M^{-1})	$\Delta G°$ (kJ/mol)
1st	3.89×10^5	-31.9
2nd	3.60×10^5	-31.7
3rd	3.33×10^5	-31.6
average	$(3.61 \pm 0.23) \times 10^5$	-31.7 ± 0.1

	$\Delta H°$ (kJ/mol)	$-T\Delta S°$ (kJ/mol)
1st	-41.9	10.0
2nd	-43.1	11.3
3rd	-44.1	12.5
average	-43.0 ± 0.9	11.3 ± 1.0

Fig. S45. ITC titration plots (heat rate versus time and heat versus guest/host ratio) of **10** to **1b** in phosphate buffer (pH =7.4) at 298 K. In this titration, the concentration of host is 0.1 mM, the concentration of guest is 2.0 mM.

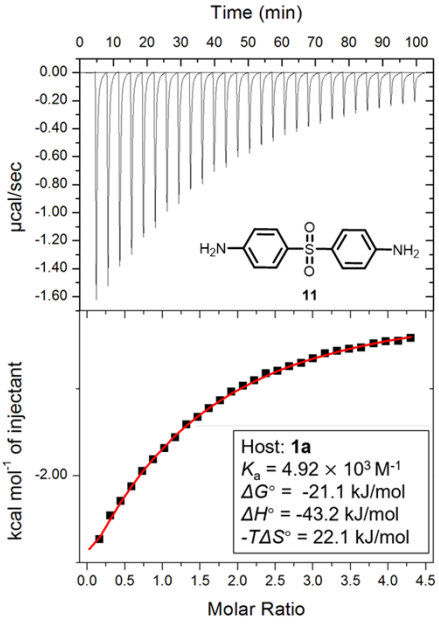

	K_a (M^{-1})	$\Delta G°$ (kJ/mol)
1st	5.55×10^3	-21.5
2nd	5.33×10^3	-21.3
3rd	4.92×10^3	-21.1
average	$(5.27 \pm 0.23) \times 10^3$	-21.3 ± 0.1

	$\Delta H°$ (kJ/mol)	$-T\Delta S°$ (kJ/mol)
1st	-34.2	12.7
2nd	-41.8	20.6
3rd	-43.2	22.1
average	-39.7 ± 4.0	18.5 ± 4.1

Fig. S46. ITC titration plots (heat rate versus time and heat versus guest/host ratio) of **11** to **1a** in phosphate buffer (pH =7.4) at 298 K. In this titration, the concentration of host is 2.0 mM, the concentration of guest is 0.1 mM.

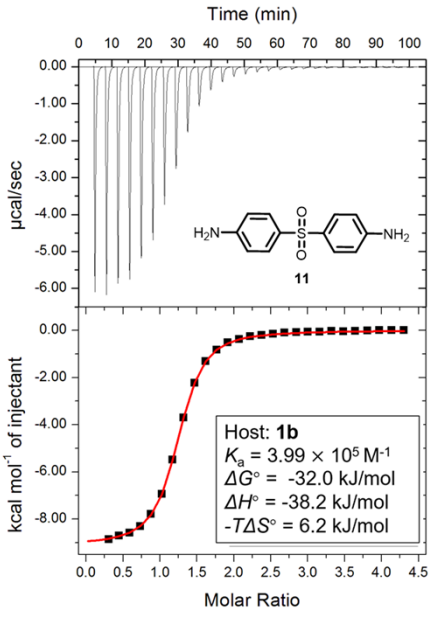

	K_a (M^{-1})	$\Delta G°$ (kJ/mol)
1st	4.47×10^5	-32.2
2nd	4.14×10^5	-32.1
3rd	3.99×10^5	-32.0
average	$(4.20 \pm 0.20) \times 10^5$	-32.1 ± 0.1

	$\Delta H°$ (kJ/mol)	$-T\Delta S°$ (kJ/mol)
1st	-42.7	10.4
2nd	-38.5	6.5
3rd	-38.2	6.2
average	-39.8 ± 2.1	7.7 ± 1.9

Fig. S47. ITC titration plots (heat rate versus time and heat versus guest/host ratio) of **11** to **1b** in phosphate buffer (pH =7.4) at 298 K. In this titration, the concentration of host is 2.0 mM, the concentration of guest is 0.1 mM.

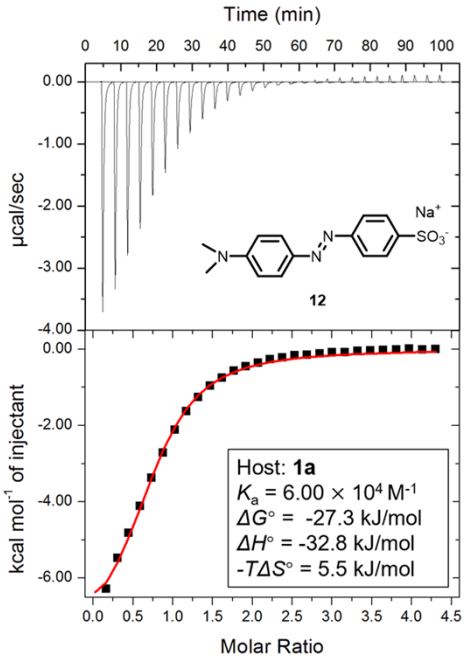

	K_a (M^{-1})	$\Delta G°$ (kJ/mol)
1st	6.00×10^4	-27.3
2nd	6.24×10^4	-27.4
3rd	5.60×10^4	-27.1
average	$(5.95 \pm 0.26) \times 10^4$	-27.3 ± 0.1

	ΔH (kJ/mol)	$-T\Delta S$ (kJ/mol)
1st	-32.8	5.5
2nd	-28.9	1.6
3rd	-28.7	1.6
average	-30.1 ± 1.9	2.9 ± 1.9

Fig. S48. ITC titration plots (heat rate versus time and heat versus guest/host ratio) of **12** to **1a** in phosphate buffer (pH =7.4) at 298 K. In this titration, the concentration of host is 0.1 mM, the concentration of guest is 2.0 mM.

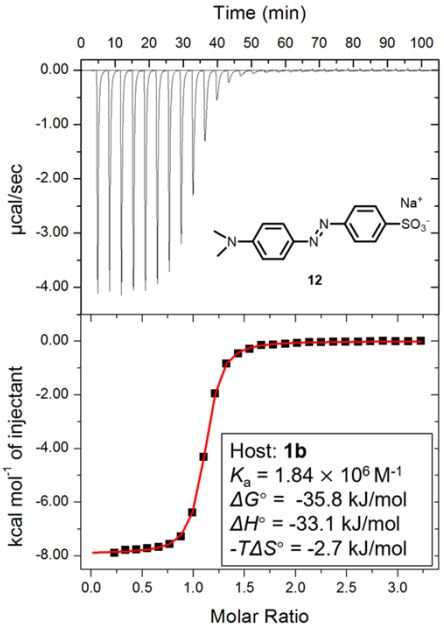

	K_a (M^{-1})	$\Delta G°$ (kJ/mol)
1st	1.92×10^6	-35.9
2nd	1.85×10^6	-35.8
3rd	1.84×10^6	-35.8
average	$(1.87 \pm 0.04) \times 10^6$	-35.8 ± 0.1

	$\Delta H°$ (kJ/mol)	$-T\Delta S°$ (kJ/mol)
1st	-34.2	-1.6
2nd	-33.3	-2.5
3rd	-33.1	-2.7
average	-33.6 ± 0.5	-2.3 ± 0.4

Fig. S49. ITC titration plots (heat rate versus time and heat versus guest/host ratio) of **12** to **1b** in phosphate buffer (pH =7.4) at 298 K. In this titration, the concentration of host is 0.1 mM, the concentration of guest is 1.5 mM.

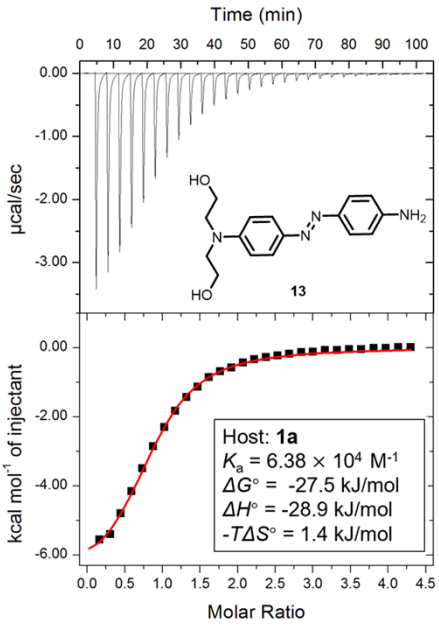

	K_a (M^{-1})	$\Delta G°$ (kJ/mol)
1st	5.71×10^4	-27.2
2nd	6.45×10^4	-27.5
3rd	6.38×10^4	-27.4
average	$(6.18 \pm 0.33) \times 10^4$	-27.3 ± 0.1

	$\Delta H°$ (kJ/mol)	$-T\Delta S°$ (kJ/mol)
1st	-28.4	1.3
2nd	-28.2	0.8
3rd	-28.9	1.4
average	-28.5 ± 0.3	1.2 ± 0.3

Fig. S50. ITC titration plots (heat rate versus time and heat versus guest/host ratio) of **13** to **1a** in phosphate buffer (pH =7.4) at 298 K. In this titration, the concentration of host is 2.0 mM, the concentration of guest is 0.1 mM.

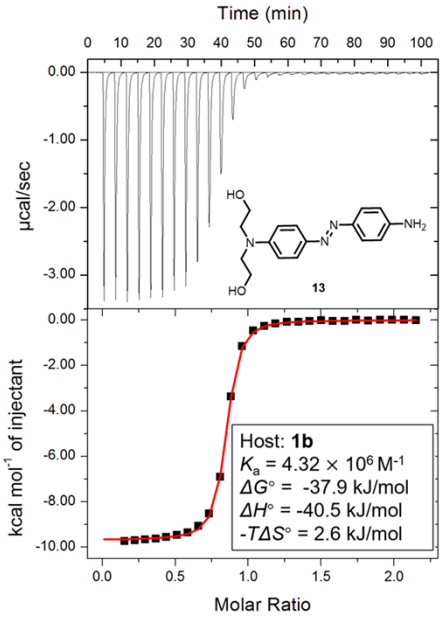

	K_a (M^{-1})	$\Delta G°$ (kJ/mol)
1st	4.28×10^6	-37.8
2nd	4.32×10^6	-37.9
3rd	3.97×10^6	-37.7
average	$(4.19 \pm 0.16) \times 10^6$	-37.8 ± 0.1

	$\Delta H°$ (kJ/mol)	$-T\Delta S°$ (kJ/mol)
1st	-40.4	2.5
2nd	-40.5	2.6
3rd	-40.4	2.7
average	-40.4 ± 0.1	2.6 ± 0.1

Fig. S51. ITC titration plots (heat rate versus time and heat versus guest/host ratio) of **13** to **1b** in phosphate buffer (pH =7.4) at 298 K. In this titration, the concentration of host is 1.0 mM, the concentration of guest is 0.1 mM.

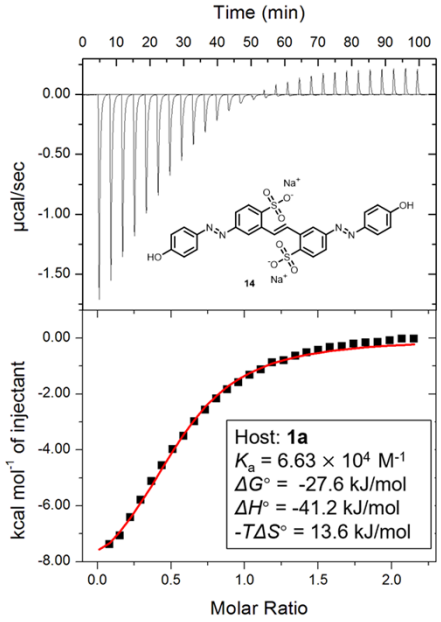

	K_a (M^{-1})	$\Delta G°$ (kJ/mol)
1st	6.63×10^4	-27.6
2nd	8.85×10^4	-28.3
3rd	7.15×10^4	-27.7
average	$(7.54 \pm 0.95) \times 10^4$	-27.9 ± 0.3

	$\Delta H°$ (kJ/mol)	$-T\Delta S°$ (kJ/mol)
1st	-41.2	13.6
2nd	-44.7	16.5
3rd	-39.9	12.2
average	-41.9 ± 2.0	14.1 ± 1.8

Fig. S52. ITC titration plots (heat rate versus time and heat versus guest/host ratio) of **14** to **1a** in phosphate buffer (pH =7.4) at 298 K. In this titration, the concentration of host is 0.1 mM, the concentration of guest is 1.0 mM.

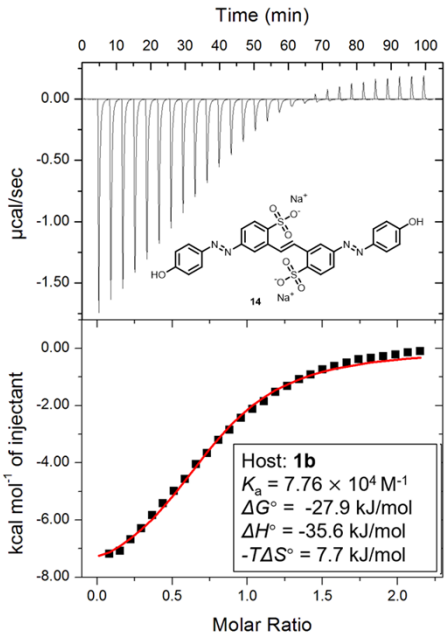

	K_a (M^{-1})	$\Delta G°$ (kJ/mol)
1st	7.76×10^4	-27.9
2nd	9.28×10^4	-28.4
3rd	8.93×10^4	-28.3
average	$(8.66 \pm 0.65) \times 10^4$	-28.2 ± 0.2

	$\Delta H°$ (kJ/mol)	$-T\Delta S°$ (kJ/mol)
1st	-35.6	7.7
2nd	-36.1	7.7
3rd	-36.5	8.3
average	-36.1 ± 0.4	7.9 ± 0.3

Fig. S53. ITC titration plots (heat rate versus time and heat versus guest/host ratio) of **14** to **1b** in phosphate buffer (pH =7.4) at 298 K. In this titration, the concentration of host is 0.1 mM, the concentration of guest is 1.0 mM.

4. Job plots

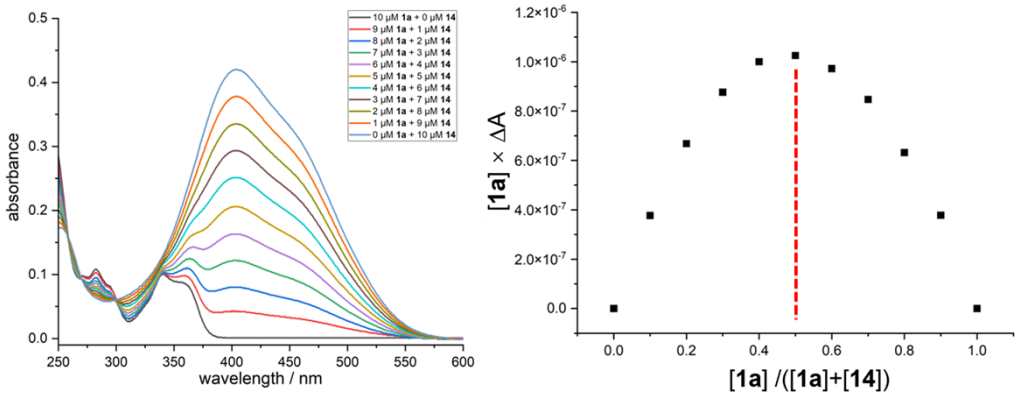

Fig. S54. Job plot of **1a** and **14** constructed from the UV-vis absorption change (λ = 403 nm) of **1a** by varying the ratio of **1a** and **14** with a fixed total concentration ([**1a**] + [**14**] = 10 μM). This experiment supports the 1:1 binding stoichiometry between **1a** and **14** in phosphate buffer (10 mM, pH = 7.4).

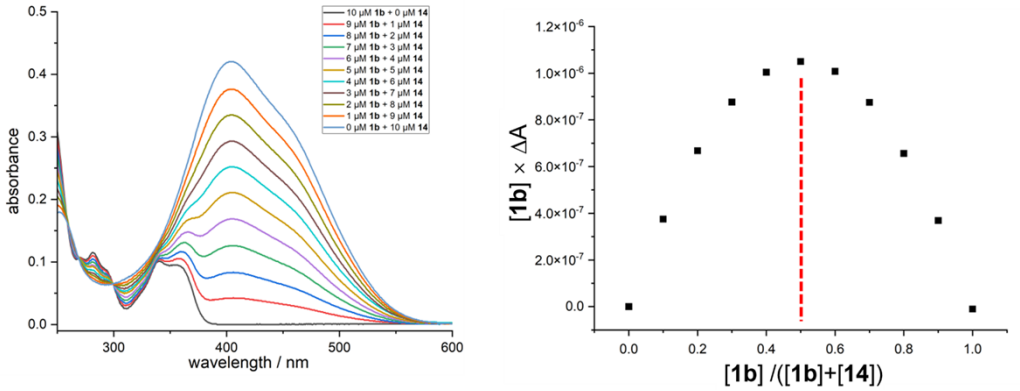

Fig. S55. Job plot of **1b** and **14** constructed from the UV-vis absorption change (λ = 403 nm) of **1b** by varying the ratio of **1b** and **14** with a fixed total concentration ([**1b**] + [**14**] = 10 μM). This experiment supports the 1:1 binding stoichiometry between **1b** and **14** in phosphate buffer (10 mM, pH = 7.4).

5. Binding Constants of CB7 by ITC titration

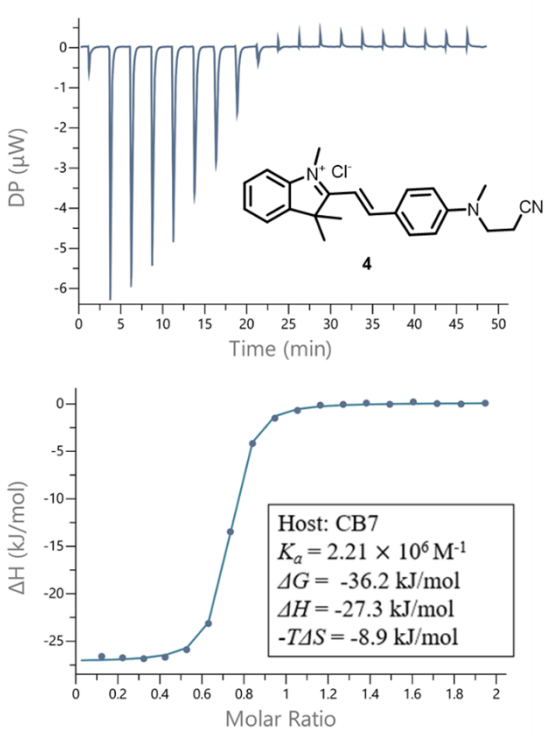

Fig. S56. ITC titration plots (heat rate versus time and heat versus guest/host ratio) of **4** (1.0 mM) to **CB7** (0.1 mM) in phosphate buffer (pH =7.4) at 298 K.

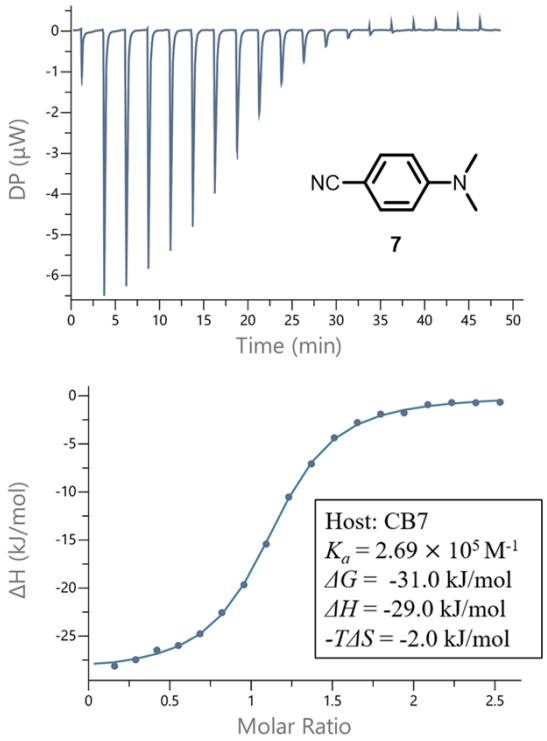

Fig. S57. ITC titration plots (heat rate versus time and heat versus guest/host ratio) of **7** (1.3 mM) to **CB7** (0.1 mM) in phosphate buffer (pH =7.4) at 298 K.

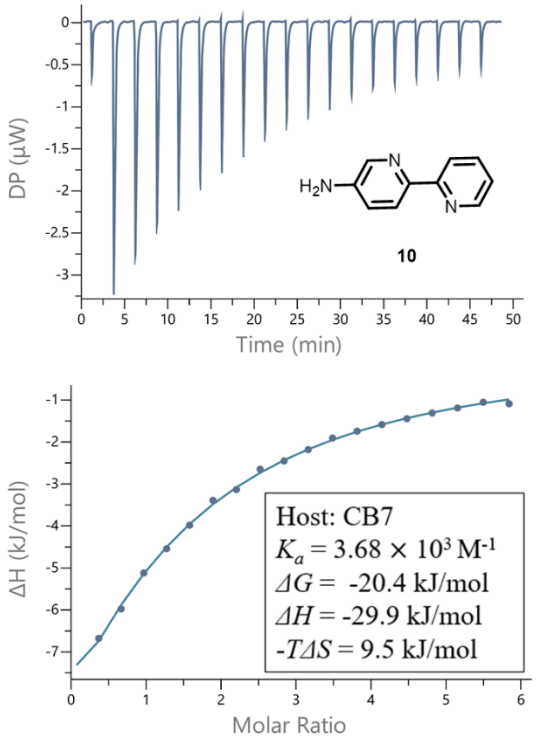

Fig. S58. ITC titration plots (heat rate versus time and heat versus guest/host ratio) of **10** (3.0 mM) to **CB7** (0.1 mM) in phosphate buffer (pH =7.4) at 298 K.

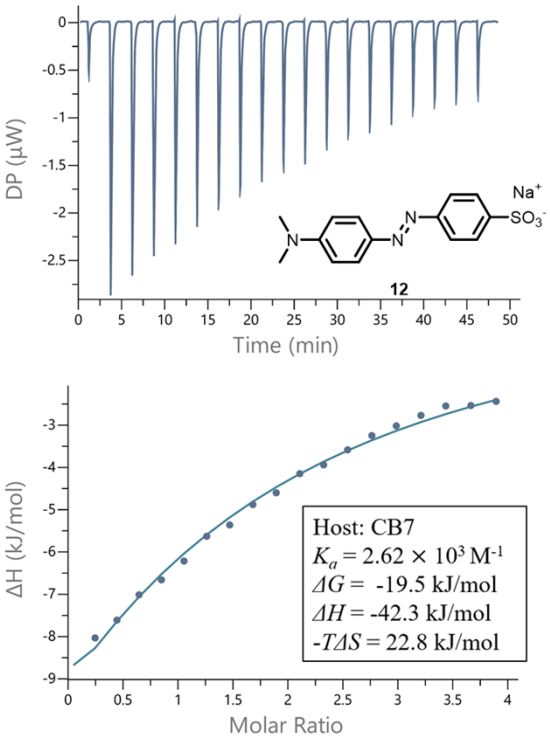

Fig. S59. ITC titration plots (heat rate versus time and heat versus guest/host ratio) of **12**(2.0 mM) to **CB7** (0.1 mM) in phosphate buffer (pH =7.4) at 298 K.

6. Binding Constants of β-CD by UV-vis titration

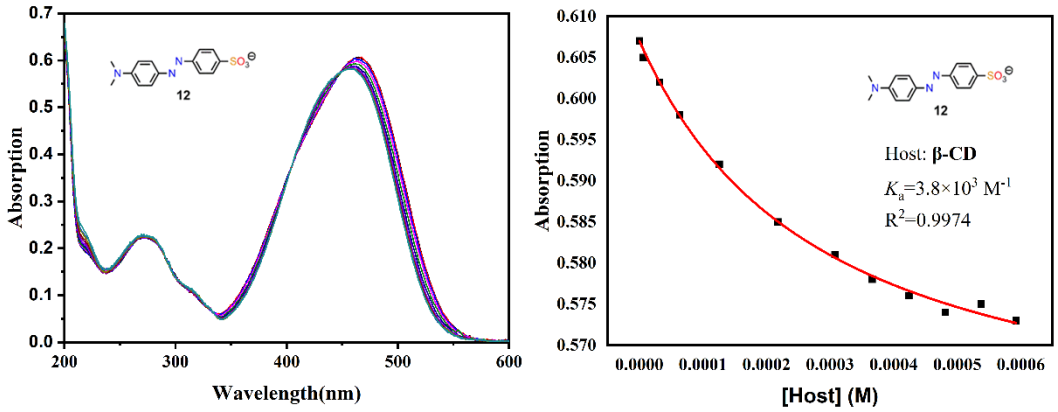

Fig. S60. UV-vis titration of ***β*-CD** with **12** in pure water at 298 K. The concentration of guest is 25 μM.

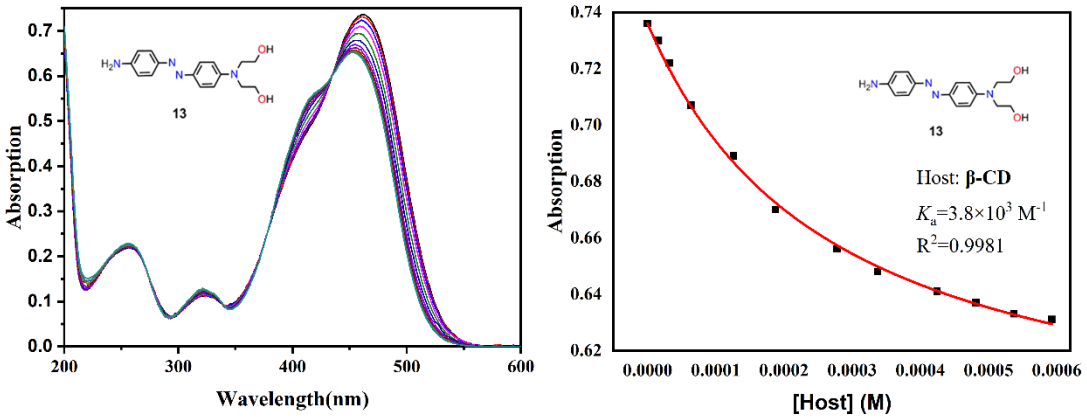

Fig. S61. UV-vis titration of ***β*-CD** with **13** in pure water at 298 K. The concentration of guest is 11.45 μM.

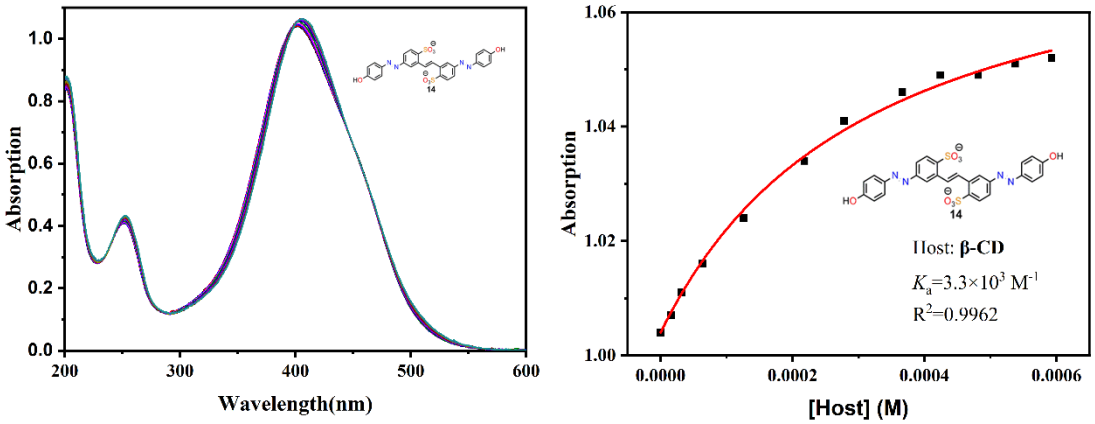

Fig. S62. UV-vis titration of **β-CD** with **14** in pure water at 298 K. The concentration of guest is 20 μM.

7. Fluorescence Quantum Yield and Lifetime

a)

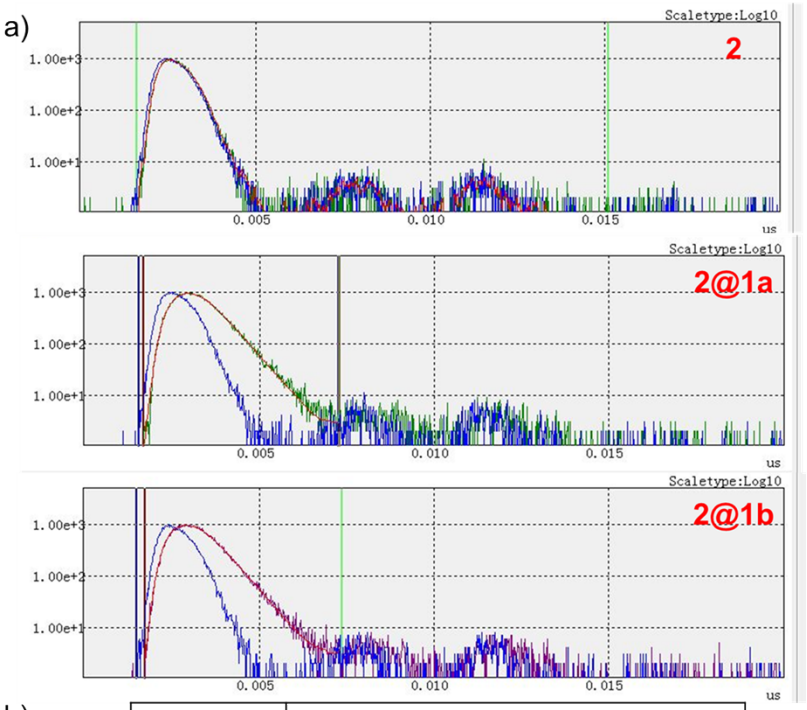

b)

sample	fluorescence quantum yield (%)
2	0.3%
2@1a	8.7%
2@1b	6.5%

Fig. S63. a) Curve fit (red line) of the fluorescence lifetime of **2** (1.0×10^{-5} M), 1:3 mixture of **2** and **1a** (1.0×10^{-5} M : 3×10^{-5} M), 1:2 mixture of **2** and **1b** (1.0×10^{-5} M : 2×10^{-5} M), excitation wavelength= 475 nm, emission wavelength= 600 nm. b) Fluorescence quantum yield of **2** (1.0×10^{-5} M), 1:3 mixture of **2** and **1a** (1.0×10^{-5} M : 3×10^{-5} M), 1:2 mixture of **2** and **1b** (1.0×10^{-5} M : 2×10^{-5} M), excitation wavelength= 475 nm.

8. UV-vis titration data for 1a and 1b

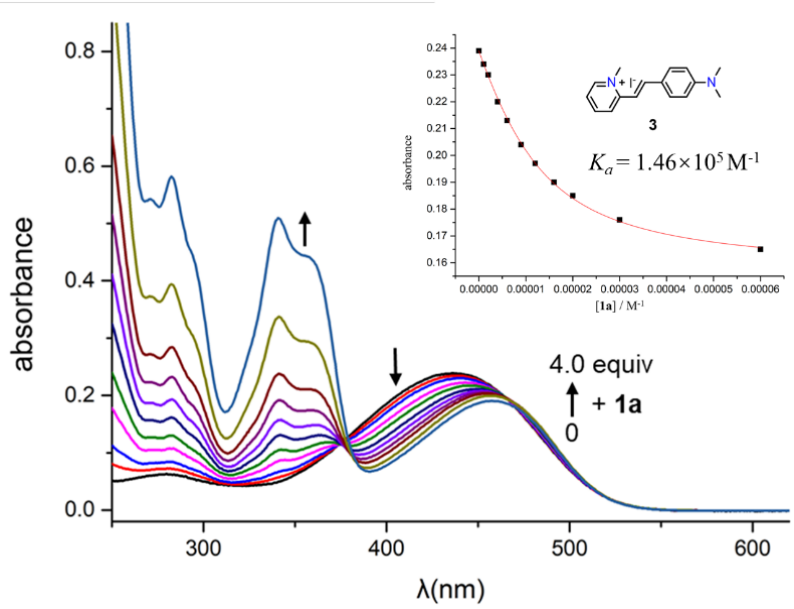

Fig. S64. UV−vis titrations of **3** with **1a** in phosphate buffer (pH =7.4) at 298 K. Inset: curve fit of the titration data at λ = 437 nm according to a 1:1 binding stoichiometry.

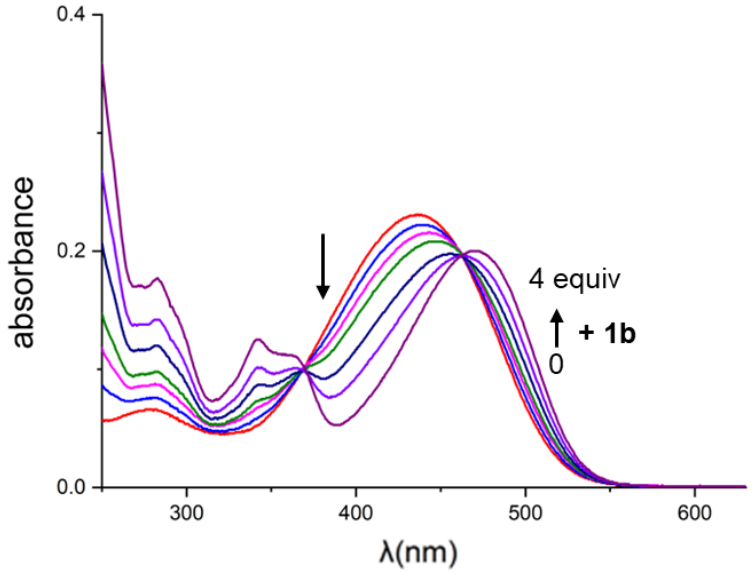

Fig. S65. UV−vis titrations of **3** with **1b** in phosphate buffer (pH =7.4) at 298 K. The titration data can't be fitted according to a 1:1 binding stoichiometry, probably because the binding constant is too high to be determined by this method (K_a = 6.3 × 10^6 M^{-1} from ITC titration).

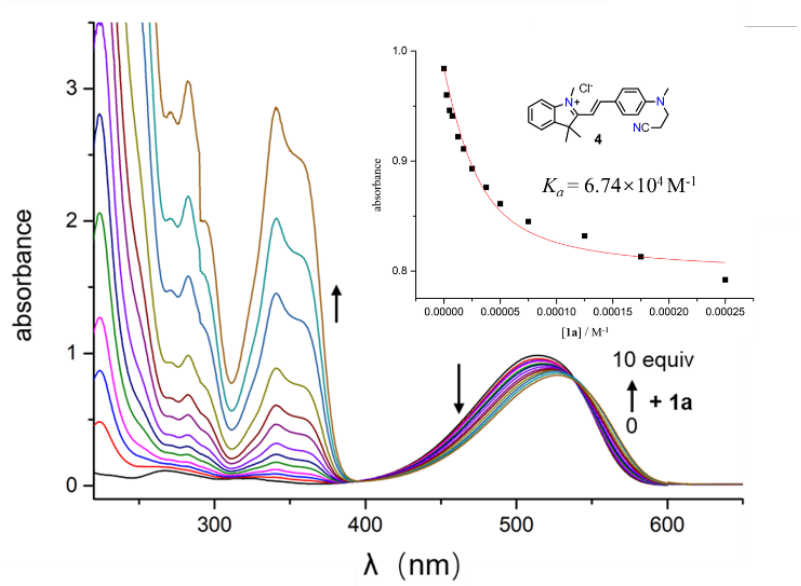

Fig. S66. UV−vis titrations of **4** with **1a** in phosphate buffer (pH =7.4) at 298 K. Inset: curve fit of the titration data at λ = 514 nm according to a 1:1 binding stoichiometry.

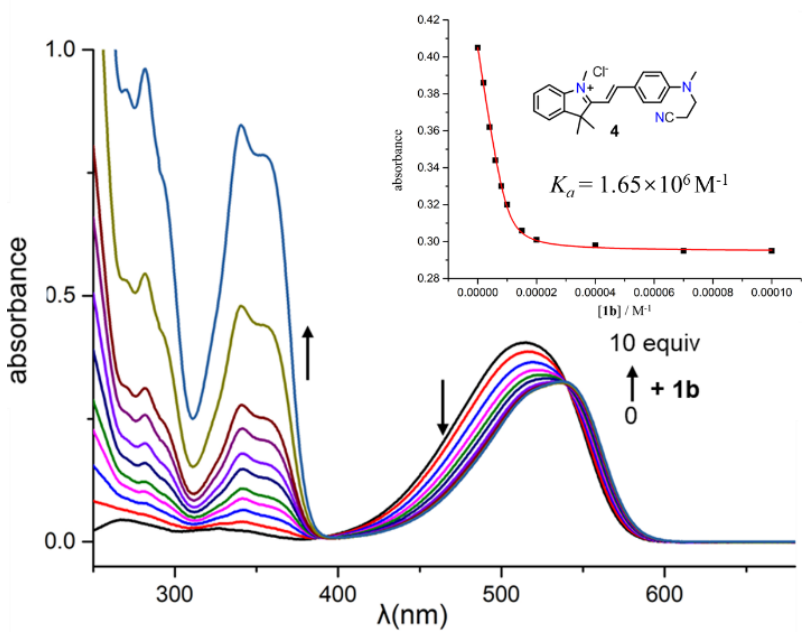

Fig. S67. UV−vis titrations of **4** with **1b** in phosphate buffer (pH =7.4) at 298 K. Inset: curve fit of the titration data at λ = 514 nm according to a 1:1 binding stoichiometry.

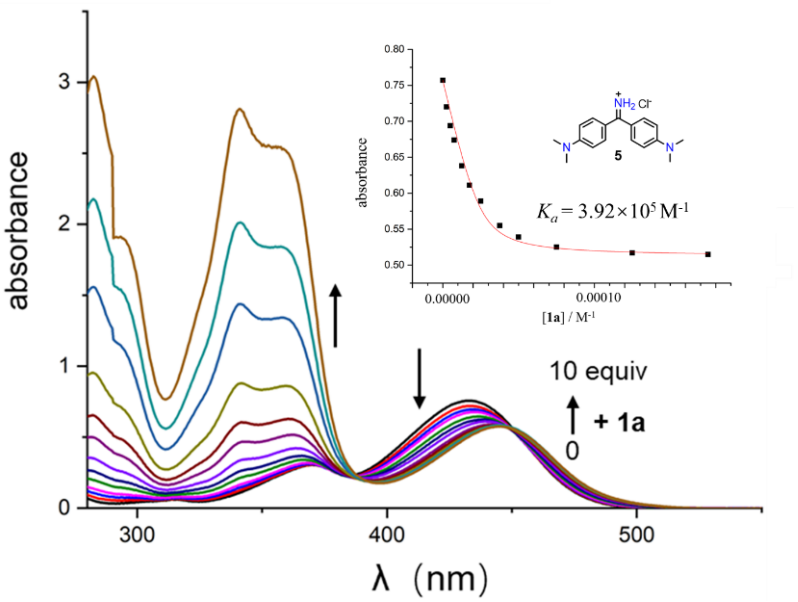

Fig. S68. UV−vis titrations of **5** with **1a** in phosphate buffer (pH =7.4) at 298 K. Inset: curve fit of the titration data at λ = 433 nm according to a 1:1 binding stoichiometry.

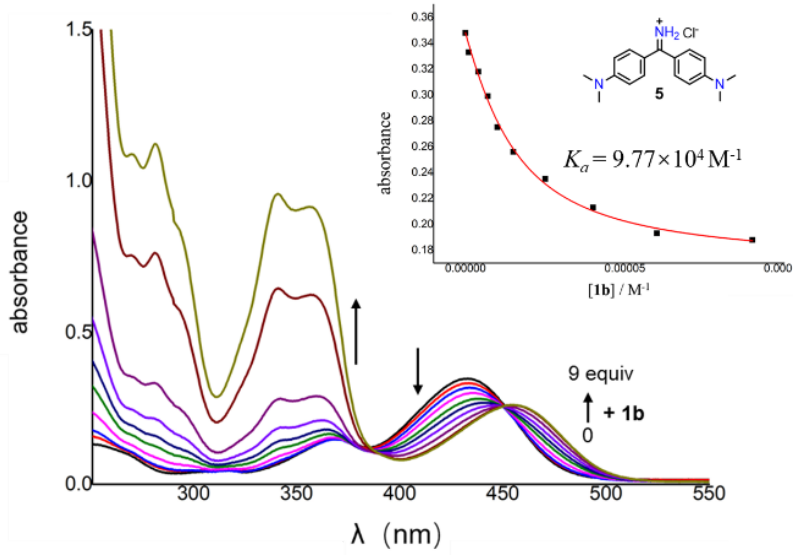

Fig. S69. UV−vis titrations of **5** with **1b** in phosphate buffer (pH =7.4) at 298 K. Inset: curve fit of the titration data at λ = 432 nm according to a 1:1 binding stoichiometry.

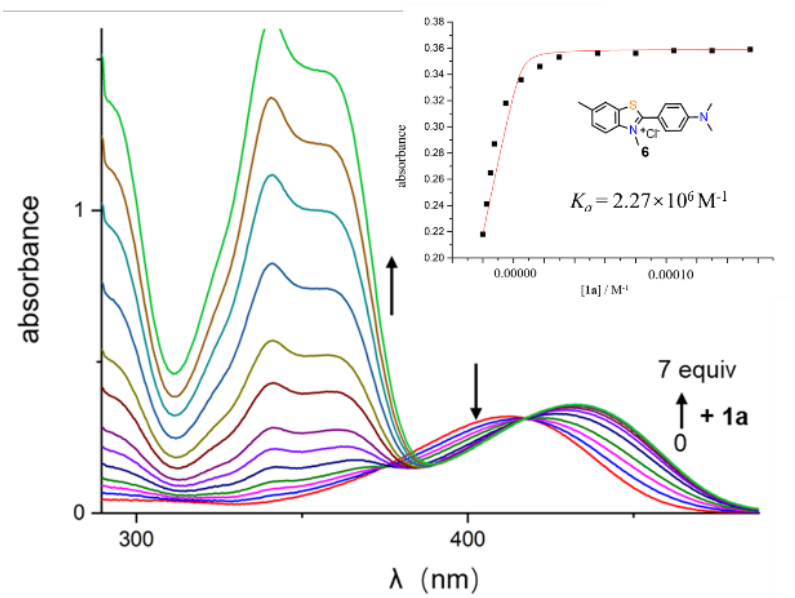

Fig. S70. UV−vis titrations of **6** with **1a** in phosphate buffer (pH =7.4) at 298 K. Inset: curve fit of the titration data at λ = 434 nm according to a 1:1 binding stoichiometry. Note: this UV-Vis fitting is not so good and the obtained constant is one order of magnitude higher than that from ITC titration (*Fig. S36*, 9.4 × 10^4 M^{-1}), and the ITC experiments are meant to be trusted as they are well-fitted and repeated three times.

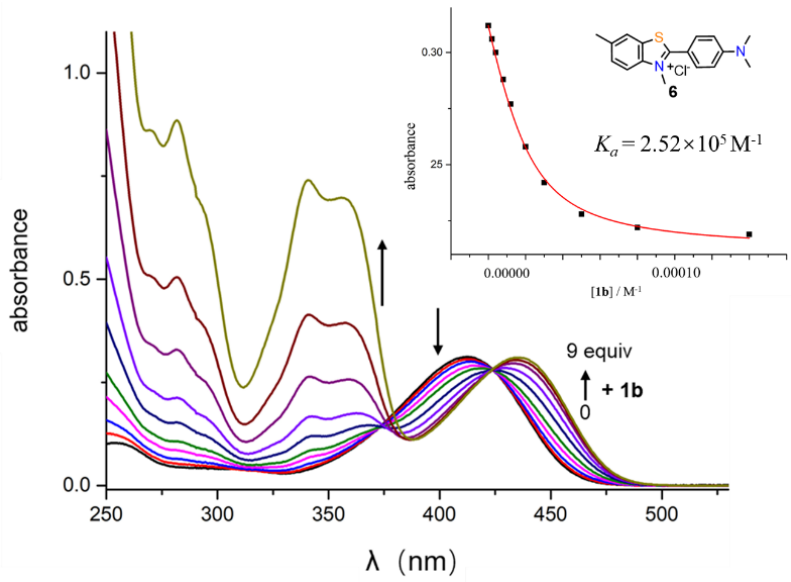

Fig. S71. UV−vis titrations of **6** with **1b** in phosphate buffer (pH =7.4) at 298 K. Inset: curve fit of the titration data at λ = 412 nm according to a 1:1 binding stoichiometry.

9 Fluorescence titration data for 1a and 1b

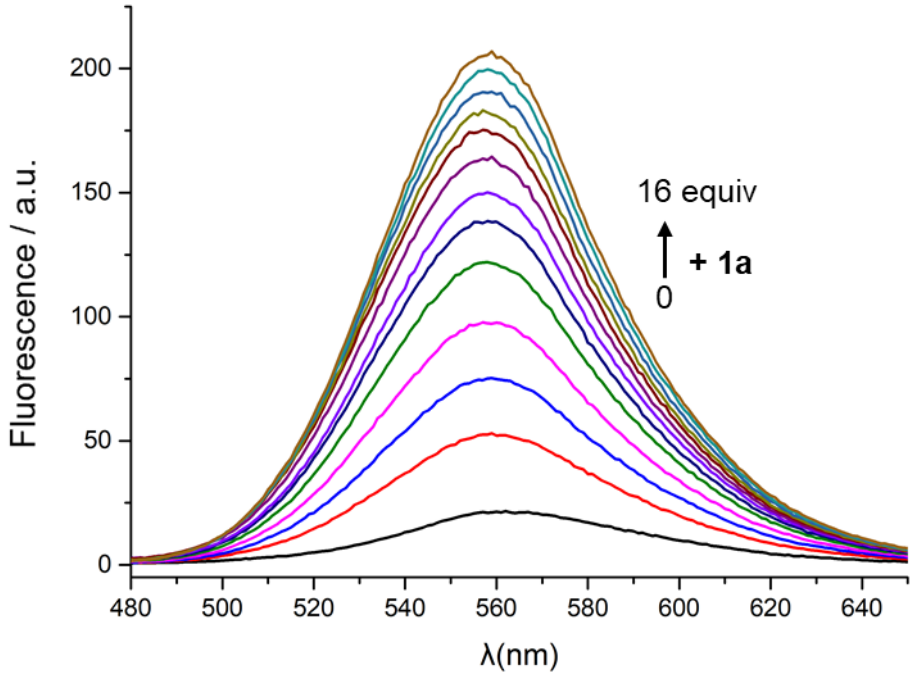

Fig. S72. Fluorescence titration of **3** with **1a**. The addition of **1a** enhanced the fluorescence intensity of **3** for 8 times.

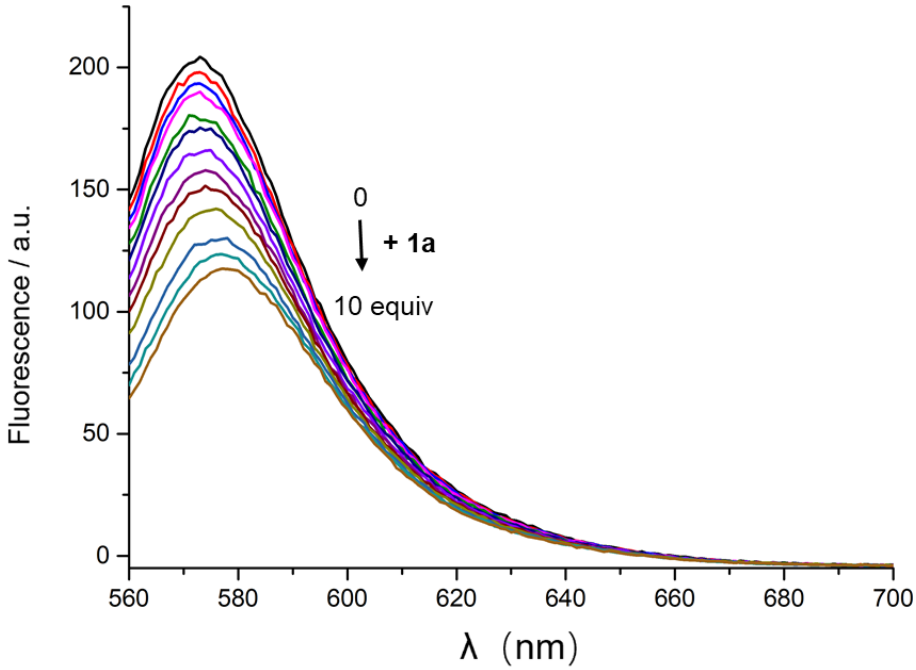

Fig. S73. Fluorescence titration of **4** with **1a**. The addition of **1a** quenched the fluorescence intensity of **4**.

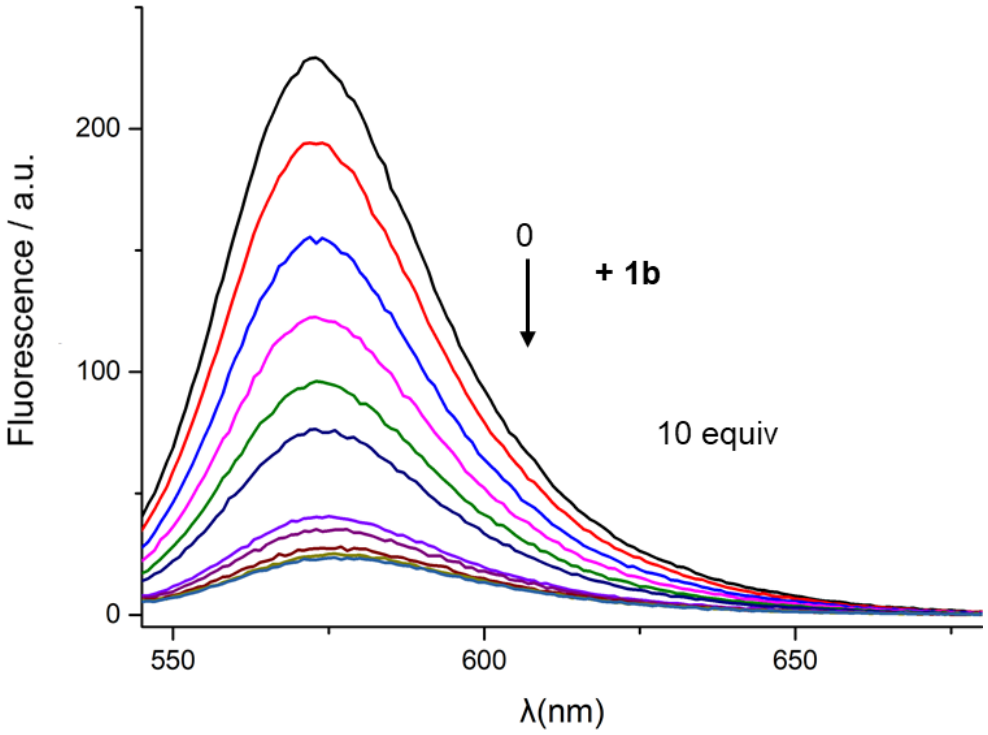

Fig. S74. Fluorescence titration of **4** with **1b**. The addition of **1b** quenched the fluorescence intensity of **4**.

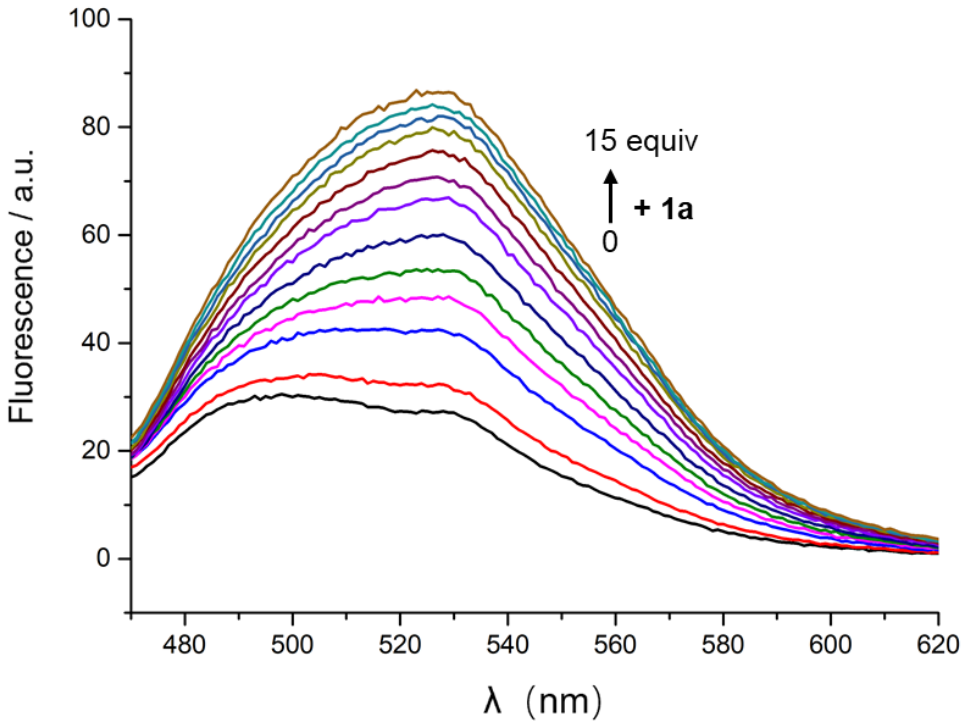

Fig. S75. Fluorescence titration of **5** with **1a**. The addition of **1a** enhanced the fluorescence intensity of **5** for 3 times.

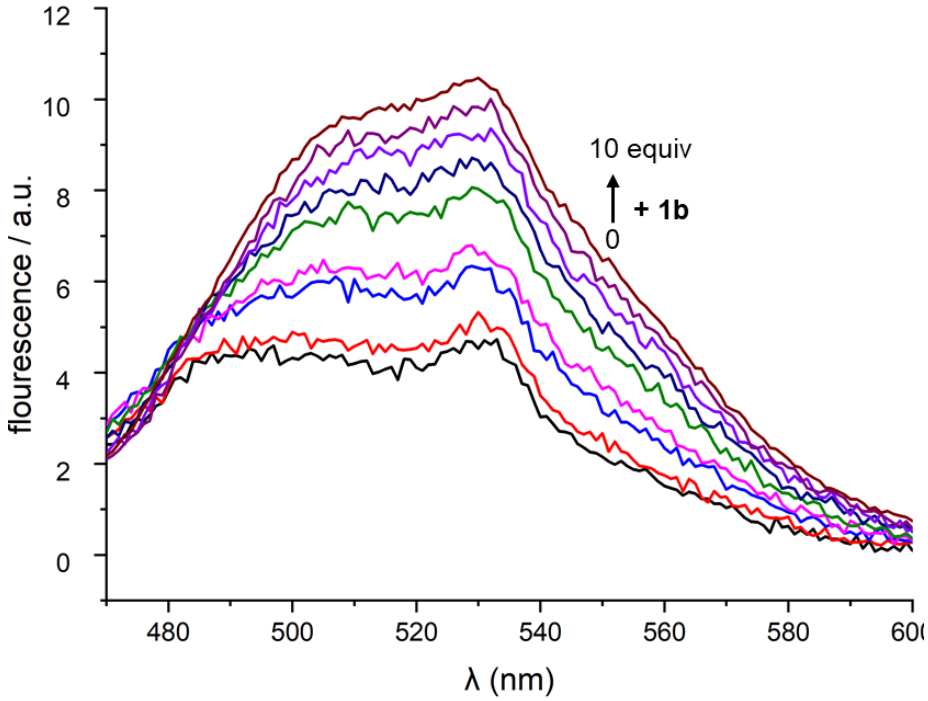

Fig. S76. Fluorescence titration of **5** with **1b**. The addition of **1b** enhanced the fluorescence intensity of **5** for about 3 times.

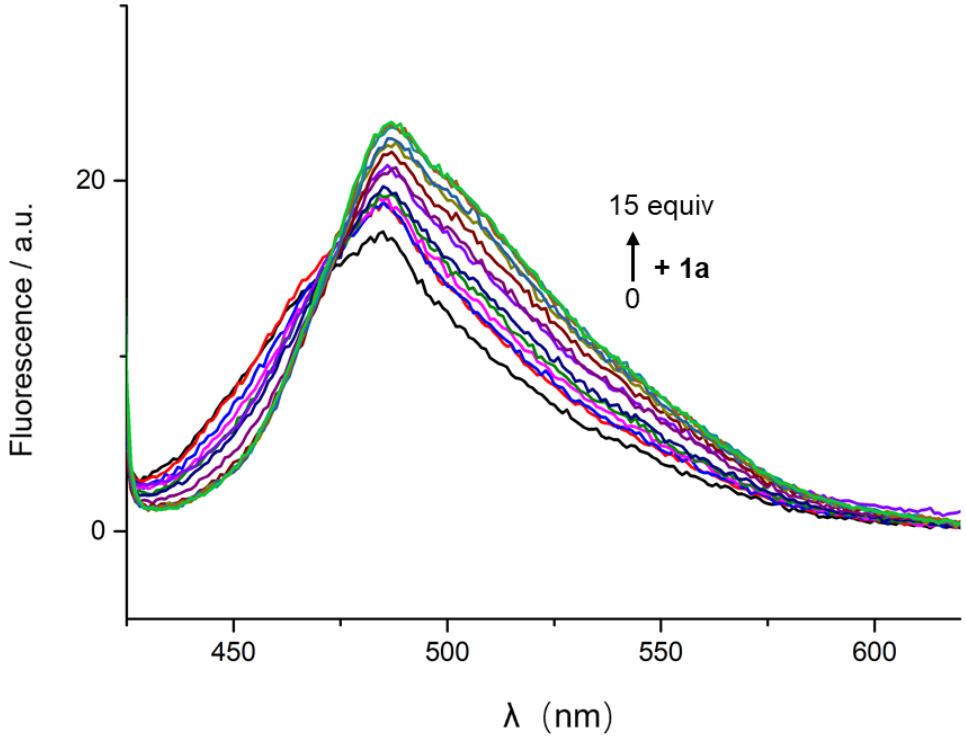

Fig. S77. Fluorescence titration of **6** with **1a**. The addition of **1a** enhanced the fluorescence intensity of **6** for less than 2 times.

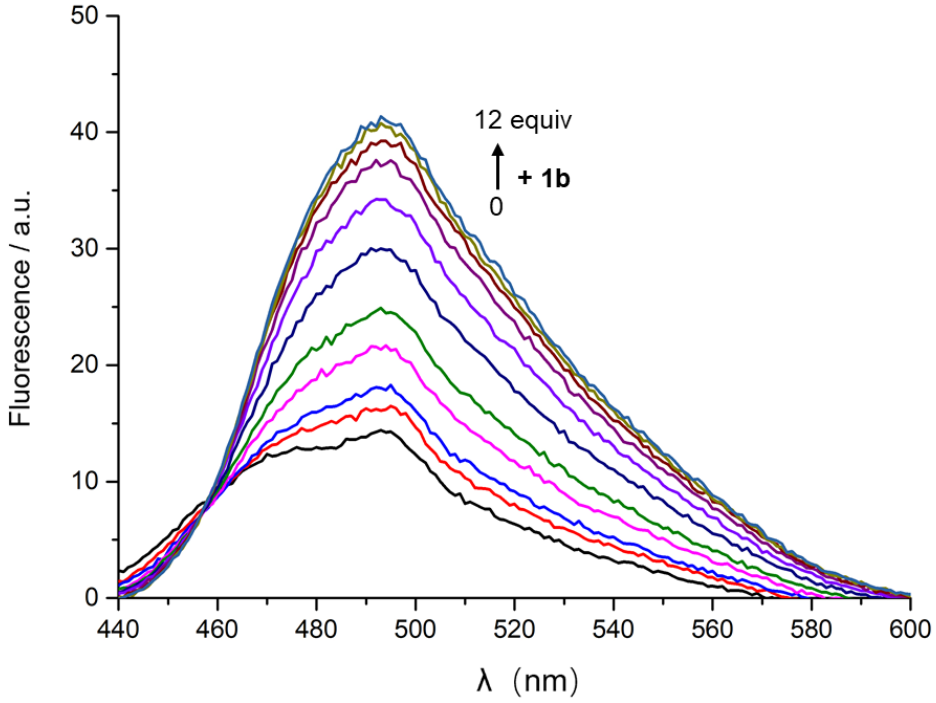

Fig. S78. Fluorescence titration of **6** with **1b**. The addition of **1b** enhanced the fluorescence intensity of **6** for about 3 times.

10. Computational data

Computational Methods. Quantum chemistry calculations were performed by using Gaussian 09 package.[3] The two representative conformation of complexes **2@1a** and **2@1b** have been optimized employing density functional theory (DFT) with dispersion corrected method (B3LYP-D3(BJ))[4] in combination with 6-31G* basis set (the Polarizable Continuum Model (PCM) water model was used).[5] Minima were identified by the absence of imaginary frequencies. Single point energy in vacuum were calculated using B3LYP-D3(BJ) method with ma-def2-TZVP basis set with the same water model.[6] The total Gibbs free energy of the complex in water is the addition of single point energy and the thermal correction to Gibbs free energy (ZPE+△G0→T). Independent gradient model based on Hirshfeld partition (IGMH) analysis[7] for the more energetically stable conformer were carried out with Multiwfn 3.8 (dev) program.[8] Molecular plots were visualized by the VMD 1.9.3 program.[9]

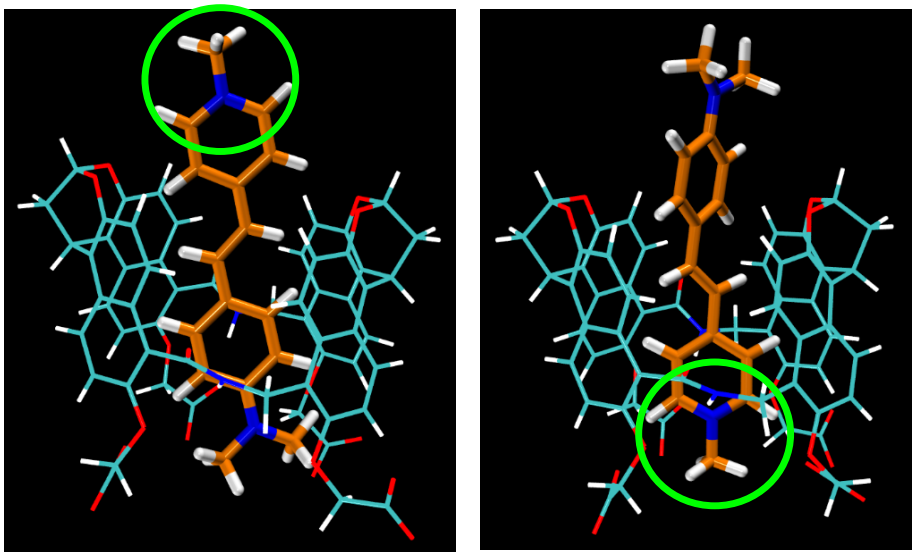

Fig. S79. Energy-minimized structures of two representative conformers of **2@1a**. The results show that **2@1a**-conformer 2 is more energetically stable than **2@1a**-conformer 1.

Cartesian coordinates of **2@1a**-conformer 2:

N	5.88788246	-0.25275902	0.85854706
C	6.03273446	-0.11790001	2.19951517

C	6.03898945	-1.22441409	3.02252823
C	5.95944548	-2.51993019	2.47040919
C	5.88913746	-2.60805120	1.06676208
C	5.83263143	-1.47797011	0.28657602
C	5.92242747	-3.74470629	3.24177725
C	5.46557642	-3.86736130	4.50989335
C	5.36766741	-5.13069039	5.21996640
C	5.93635044	0.94533307	0.00049500
C	6.14946245	-6.24545848	4.87094937
C	6.02659844	-7.46093459	5.51655143
C	5.09542339	-7.63609560	6.57159751
C	4.30979333	-6.51467751	6.93236955
C	4.45916034	-5.30135139	6.27712847
N	4.97087738	-8.84642869	7.22120455
C	3.89061530	-9.03733070	8.17603964
C	5.61803741	-10.02440275	6.66365149
H	6.10717949	0.90682607	2.55081220
H	6.14328547	-1.07639108	4.08970731
H	5.82748344	-3.57178528	0.58460405
H	5.69012241	-1.49106312	-0.78937006
H	6.17741248	-4.64168336	2.68522121
H	5.08393039	-2.98922923	5.02680638
H	5.51835941	0.67761805	-0.96999207
H	5.37114738	1.73712513	0.48844604
H	6.98530855	1.24886910	-0.08114901
H	6.88718353	-6.14510949	4.08665431
H	6.64573551	-8.28532665	5.18788640
H	3.57746227	-6.58974850	7.72662862
H	3.83724629	-4.46730634	6.57103552
H	2.89714922	-8.93506768	7.71339760
H	3.96930730	-10.03570376	8.60773366
H	3.96042130	-8.31208963	8.99420969
H	5.27474540	-10.24502077	5.64167544
H	6.70644050	-9.89992074	6.63624450
H	5.39636644	-10.88456682	7.29609355
O	8.75237669	-0.23077202	1.15557309
O	5.13577439	-0.78670806	-2.58286620
C	9.35122870	0.87377107	1.26102310
C	4.18066232	-0.80809806	-3.40767626
C	8.88757370	-2.43240318	5.26431740
C	9.85940777	-0.61751205	3.94954830
C	9.65721576	-1.97884915	4.14495131
C	3.92865230	-5.99296246	0.68293605
C	3.59514828	-6.26645750	1.99613115

C	1.72241913	-1.47814511	1.14667509
C	2.44264019	-2.52819119	0.33216703
C	2.77535921	-2.25484817	-0.99223208
C	7.36353158	-3.27830725	7.47697956
C	7.37413656	-1.92942015	7.17470156
C	6.45160948	-1.03351208	8.00112460
C	8.19906563	-1.47805811	6.09260447
C	8.78356968	-3.81142829	5.59965443
C	8.07838062	-4.21670232	6.70221851
C	8.40644665	-0.10185701	5.81548646
C	9.22418272	0.32132202	4.79478037
O	10.76670783	-0.24059902	2.99841923
C	10.53914082	0.95648507	2.24859617
O	9.11547172	1.94011915	0.64525305
C	4.21338832	-2.14622116	7.88950159
C	5.03703038	-1.13496409	7.43349956
C	4.57397135	-0.32424002	6.34918648
C	3.41330426	-0.71387105	5.60175240
C	2.60737820	-1.76505313	6.12243546
C	2.96624823	-2.41142718	7.27823255
C	5.21377440	0.88694207	5.98387145
C	4.81486737	1.61667513	4.89298037
C	3.79938029	1.12193009	4.03898531
C	3.10459123	-0.03302200	4.37929534
O	3.50153927	1.72623313	2.85315922
C	3.58925327	3.16226224	2.76931921
C	4.97879338	3.77470429	2.45590119
O	4.92854938	5.00566938	2.22418917
C	10.24339979	-3.51859527	0.73199306
O	6.66555753	-3.82451729	8.53366964
O	4.53764535	-2.98576223	8.93312470
C	6.44227151	-1.56978612	9.43642571
C	5.88935145	-2.98053523	9.37365370
C	2.84419722	-5.35308842	2.76919221
C	2.47717419	-4.13740832	2.24399017
C	2.77439221	-3.80086729	0.89290407
C	3.44467626	-4.78675337	0.09005901
C	3.27887525	-3.28606625	-1.82388414
C	3.59308827	-4.51025334	-1.29219610
O	2.56512120	-0.98905708	-1.45110511
C	2.73018921	-0.73414806	-2.85110422
O	4.23582633	-0.85172206	-4.65724635
C	8.05392760	-6.98179354	2.13474416
C	8.78197167	-5.92989146	1.63971613

C	8.33353465	-5.20811740	0.49543504
C	7.12322754	-5.64688641	-0.14504401
C	6.31306548	-6.66794952	0.45330303
C	9.03919870	-4.07247931	-0.00183000
C	8.56101466	-3.40007926	-1.12516808
C	7.44574355	-3.91185430	-1.83224914
C	6.76010653	-5.00146338	-1.35296911
O	9.20038371	-2.26122017	-1.48607711
C	8.68053268	-1.47259411	-2.56709720
C	8.96566169	-2.02924216	-3.98790430
O	9.61008475	-3.10200824	-4.08090131
C	4.88141037	-6.96946853	-0.00026200
C	4.49621434	-8.37866865	0.46317304
O	3.97098030	-7.41979355	2.65134620
C	6.79637650	-7.31121955	1.57717812
C	4.71924336	-8.41809966	1.96295215
O	6.09968147	-8.28581963	2.26333217
H	0.85497507	-1.90538715	1.65435113
N	2.55121720	-0.88908507	2.19731717
O	10.85462582	-3.97813330	3.48143027
N	9.84791177	-2.70007021	1.87380314
O	5.99178043	3.02373423	2.47966019
O	8.49946463	-1.30293710	-4.90524238
H	1.36124110	-0.69145105	0.47957404
H	6.80294153	-0.00229500	8.00713463
H	9.30136872	-4.53705635	4.98749438
H	8.00763264	-5.26481040	6.97064055
H	7.95503263	0.64750705	6.45029548
H	9.39175172	1.38225611	4.65263336
H	10.41295279	1.82662914	2.90151022
H	11.46277287	1.10853809	1.68322213
H	1.68853813	-2.02283115	5.61342743
H	2.33697618	-3.18471824	7.70742758
H	6.01836847	1.27253810	6.59489348
H	5.34139339	2.51842919	4.61664935
H	2.90192822	3.43168326	1.96368215
H	3.20519324	3.60216428	3.69811228
H	10.89047482	-4.31292333	1.10477108
H	10.82695884	-2.90183922	0.04461900
H	7.45217957	-1.58689612	9.85543974
H	5.80314245	-0.96481107	10.08567677
H	5.86531744	-3.48117227	10.34051578
H	2.63056820	-5.60846840	3.80147529
H	1.96261815	-3.42342526	2.87695022

H	3.43066626	-3.11349124	-2.88095822
H	3.94664630	-5.28433340	-1.96034615
H	2.08379516	-1.40012211	-3.43422326
H	2.36162318	0.28733902	-2.98422423
H	8.39375565	-7.54144859	3.00062723
H	9.68860274	-5.62810040	2.15118716
H	7.11707855	-3.43485126	-2.74533021
H	5.91777648	-5.36388342	-1.92016615
H	7.60430760	-1.30328210	-2.44489019
H	9.18011267	-0.50548704	-2.45612519
H	4.80008836	-6.91298351	-1.08551708
H	3.44862926	-8.59069066	0.23181302
H	5.12106539	-9.14422070	-0.00542700
H	4.42767534	-9.36089269	2.42384819
H	3.45876326	-0.52882304	1.93832615
H	9.40769974	-1.78832014	1.66297313
O	0.94550007	-0.95113807	3.80630729
C	2.08715916	-0.63251505	3.44467927
C	10.20155875	-2.97338323	3.14358324

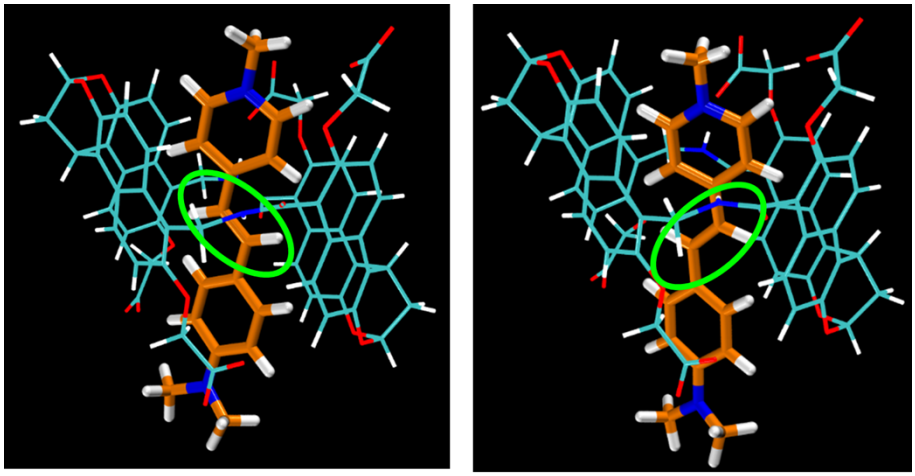

Fig. S80. Energy-minimized structures of two representative conformers of **2@1b**. The results show that **2@1b**-conformer 2 is more energetically stable than **2@1b**-conformer 1.

Cartesian coordinates of **2@1b**-conformer 2

C	-5.63239900	18.85218600	3.38455600
C	-6.08581000	16.58034800	2.65693300
C	-7.31052600	16.66747700	3.35578200
C	-7.64492900	17.81792900	4.02253400

C	-5.62302300	15.38865700	1.99675500
C	-6.37413000	14.27688100	1.78372800
C	-5.88520500	13.01976200	1.27784500
C	-4.50610500	12.74569000	1.15742700
C	-4.04272300	11.50301700	0.78807000
C	-4.94619900	10.44275100	0.50865700
C	-6.33212000	10.73180300	0.57040800
C	-6.78330400	11.98530700	0.95466200
N	-4.47542500	9.18668000	0.20464200
C	-5.41657400	8.09302000	0.02277900
C	-3.08730000	8.86084700	0.51903500
C	-2.02156500	16.56522400	3.27324100
C	-2.30354900	18.87843300	4.01558500
C	-2.29677400	17.52140800	4.28999300
C	-1.46812400	14.70731600	1.24955800
C	-1.63710600	16.03193300	0.88560900
C	-1.73568400	16.33148100	-0.60680900
C	-1.81169800	17.00361600	1.92297100
C	-1.94313300	15.17484700	3.56476500
C	-1.61700900	14.27438700	2.58580100
C	-1.77739100	18.40585800	1.69693100
C	-2.00682300	19.31998200	2.70237500
O	-2.63388700	19.70912800	5.04024700
C	-2.26927700	21.09465000	4.96084300
C	-3.23927200	22.02702600	4.19013200
O	-4.26216700	21.52580400	3.64951800
C	-3.41993400	14.69379700	-1.46446400
C	-3.15364700	15.99700500	-1.08192200
C	-4.23970800	16.93449200	-1.07431000
C	-5.57502400	16.49189500	-1.36821500
C	-5.78314900	15.12157900	-1.68940800
C	-4.72745300	14.25508000	-1.76614100
C	-4.05603700	18.31591800	-0.80820200
C	-5.10206200	19.21000600	-0.82143100
C	-6.41882700	18.76498700	-1.07995000
C	-6.65814400	17.42017000	-1.31614600
O	-7.47652700	19.62265000	-1.21253800
C	-7.56410800	20.75511100	-0.34443700
C	-7.89074100	20.40974300	1.12772700
O	-8.12180300	19.20512500	1.41706800
O	-1.18948400	13.69561500	0.35455700
O	-2.45861500	13.71083700	-1.57661000
C	-0.74835200	15.40945700	-1.33106600
C	-1.17827300	13.98409100	-1.03829800

C	-2.64727000	17.00423800	5.66104400
N	-3.92295400	16.55481100	5.73143400
O	-1.85408300	16.93280500	6.60188800
C	-8.07115300	16.91182500	-1.46315500
N	-8.84366100	17.16147100	-0.38550000
O	-8.44173600	16.25620600	-2.44911700
O	-4.69208700	13.36742300	5.35318400
O	-10.32636300	18.17045500	7.70678200
C	-5.85604400	13.97866900	5.69205200
C	-5.76205300	15.15444700	6.43578100
C	-6.93732400	15.89196600	6.75988400
C	-8.23186900	15.40560000	6.36533200
C	-8.27214500	14.16795700	5.67754700
C	-7.13179400	13.47840900	5.33470000
C	-6.86998400	17.13251300	7.45492100
C	-8.00828500	17.83072200	7.76225000
C	-9.27331700	17.35217000	7.35277700
C	-9.41225200	16.17195800	6.64322800
C	-4.39450100	15.66887400	6.79912200
C	-4.73936200	12.07696800	4.72486700
C	-3.32555800	11.47579900	4.52068900
O	-3.36537300	10.30813400	4.05150800
C	-10.16894000	14.47655100	1.03436100
C	-10.35774600	15.85102000	1.03001100
C	-10.67154800	16.51710700	2.25722400
C	-10.76538300	15.76736200	3.48152800
C	-10.65705800	14.35332700	3.39850100
C	-10.36423300	13.72128100	2.21473700
C	-10.90801300	17.91807200	2.31026800
C	-11.25237800	18.53553100	3.48603500
C	-11.27820500	17.79927900	4.69005900
C	-10.97487700	16.44912900	4.72168400
O	-9.77833700	13.85037100	-0.12416300
C	-10.70222100	12.89711200	-0.68658500
C	-10.58645900	11.41513800	-0.23523100
O	-11.59360500	18.53969600	5.80824100
C	-11.57707000	17.91812500	7.08913000
C	-11.86066600	16.42983100	7.02097100
C	-10.80043500	15.81670500	6.09914500
C	-10.19063000	16.61920700	-0.26300400
O	-2.32113700	12.16886100	4.81620800
O	-11.38146300	10.66484600	-0.85464600
O	-9.75855300	11.10060900	0.66031100
O	-2.87798800	23.22706400	4.20159500

O	-7.90627500	21.40663900	1.89046100
H	-5.01674400	19.74970200	3.45232600
H	-7.99226400	15.83081600	3.40718800
H	-8.57339000	17.91988500	4.56494800
H	-4.58894800	15.41081000	1.66552000
H	-7.43443000	14.30087300	2.02807400
H	-3.78272300	13.51257400	1.39883700
H	-2.97383300	11.34742500	0.73039800
H	-7.07286400	9.97215900	0.35424900
H	-7.85821000	12.14556000	0.99383500
H	-4.87172500	7.20416400	-0.29759100
H	-5.96778600	7.85281300	0.94491000
H	-6.14637500	8.33796600	-0.75556500
H	-2.39334400	9.39760100	-0.13894000
H	-2.84530900	9.11390500	1.55986000
H	-2.93146800	7.79211600	0.36827700
H	-1.48564800	17.36968000	-0.82462600
H	-2.13695300	14.79477400	4.56067200
H	-1.54028400	13.22112200	2.83066600
H	-1.53908500	18.78311200	0.71053000
H	-1.99945200	20.37798400	2.47542400
H	-2.22697500	21.42823800	6.00133800
H	-1.26075100	21.19192900	4.54166500
H	-6.78770900	14.77328500	-1.88867600
H	-4.87000700	13.20854900	-2.01223600
H	-3.06366400	18.69756200	-0.61983600
H	-4.90509400	20.26133100	-0.64733700
H	-6.65660300	21.36690500	-0.38302300
H	-8.37809500	21.35887700	-0.75543800
H	-0.76861300	15.57008100	-2.41270000
H	0.27204200	15.56958200	-0.97187800
H	-0.52108400	13.23541300	-1.47850600
H	-4.46876800	16.56979700	4.87972600
H	-8.51804100	17.85600700	0.30664300
H	-9.22236200	13.74482300	5.39406100
H	-7.21946000	12.55217200	4.78127800
H	-5.90968500	17.54869600	7.73325100
H	-7.96558500	18.77397200	8.29716300
H	-4.39832100	16.20789900	7.74934100
H	-3.69575100	14.83397600	6.90167700
H	-5.32997600	11.38742600	5.34069500
H	-5.22158400	12.16085400	3.74544100
H	-10.84054000	13.74873700	4.27790500
H	-10.26283000	12.64372200	2.14333600

H	-10.79478700	18.52012700	1.41912600
H	-11.45534100	19.60064200	3.52692200
H	-11.72916500	13.24048600	-0.50957200
H	-10.52588300	12.93416600	-1.76617800
H	-12.30111700	18.47124500	7.68562400
H	-11.80611600	16.01474200	8.03133100
H	-12.86585200	16.25889200	6.62596900
H	-10.93505000	14.73616400	6.06373800
H	-10.33346600	15.94916200	-1.10862300
H	-10.93290300	17.42186500	-0.33815400
C	-5.26400500	17.72804000	2.68307600
H	-4.32512200	17.73529600	2.14678500
N	-6.80462400	18.87908700	4.06197600
C	-7.22869400	20.12461400	4.71983100
H	-7.80378200	19.87559200	5.61244700
H	-6.33611800	20.69182400	4.98417100
H	-7.81872100	20.69252300	3.99296000

11. CD Spectral of 15 and 3@15

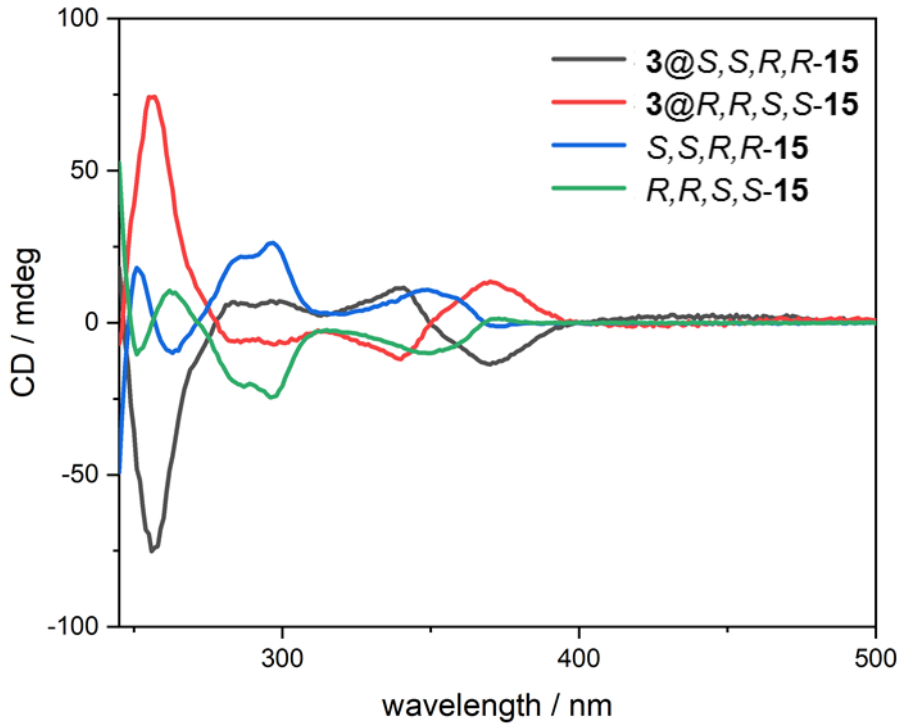

Fig. S81. CD spectra of chiral naphthotubes **15** and 1:1 mixture of **15** and **3** (50 μM) in 10 mM phosphate buffer (pH 7.4) at 25 °C.

12. Reference

1. G.-B. Huang, S.-H. Wang, H. Ke, L.-P. Yang, W. Jiang, *J. Am. Chem. Soc.* 2016, **138,** 14550-14553.

2. H. Ke, L.-P. Yang, M. Xie, Z. Chen, H. Yao, W. Jiang, *Nat. Chem.* 2019, **11**, 470-477.

3. M. J. Frisch, G. W. Trucks, H. B. Schlegel, G. E. Scuseria, M. A. Robb, J. R. Cheeseman, G. Scalmani, V. Barone, B. Mennucci, G. A. Petersson, H. Nakatsuji, M. Li, X. Caricato, H. P. Hratchian, A. F. Izmaylov, J. Bloino, G. Zheng, J. L. Sonnenberg, M. Hada, M. Ehara, K. Toyota, R. Fukuda, J. Hasegawa, M. Ishida, T. Nakajima, Y. Honda, O. Kitao, H. Nakai,. T. Vreven, J. A. Montgomery Jr., J. E. Peralta, F. Ogliaro, M. J. Bearpark, J. Heyd, E. N. Brothers, K. N. Kudin, V. N. Staroverov, R. Kobayashi, J. Normand, K. Raghavachari, A. P. Rendell, J. C. Burant, S. S. Iyengar, J. Tomasi, M. Cossi, N. Rega, N. J. Millam, M. Klene, J. E. Knox, J. B. Cross, V. Bakken, C. Adamo, J. Jaramillo, R. Gomperts, R. E. Straumann, O. Yazyev, Austin, A. J. Cammi, R. Pomelli, C. Ochterski, J. W. Martin, R. L. Morokuma, K. Zakrzewski, V. G. Voth, G. A. Salvador, P. Dannenberg, J. J. Dapprich, S. Daniels, A. D. Farkas, Ö. Foresman, J. B. Ortiz, J. V. Cioslowski, J. Fox, D. J. Gaussian 09, Gaussian, Inc.: Wallingford, CT, USA, 2013.

4. (a) S. Grimme, J. Antony, S. Ehrlich, H. A Krieg, *J. Chem. Phys.*, 2010, **132,** 154104. (b) P. J. Stephens, F. J. Devlin, C. F. Tabloski, M. J. Frisch, *J. Phys. Chem.*, 1994, **98**, 11623-11627. (c) S. Grimme, S. Ehrlich, L. Goerigk, *J. Comput. Chem.*, 2011, **32,** 1456-1465.

5. (a) E. Cances, B. Mennucci, J. Tomasi, *J. Chem. Phys.* 1997, **107**, 3032-3041. (b) B. Mennucci, J. Tomasi, *J. Chem. Phys.* 1997, **106,** 5151-5158.

6. (a) F. Weigend, R. Ahlrichs, *Phys. Chem. Chem. Phys.*, 2005, **7**, 3297-3305. (b) J. Zheng, X. Xu, D. G. Truhlar, *Theor. Chem. Acc.*, 2011, **128**, 295-305.

7. T. Lu, Q. Chen, *J. Comput. Chem.,* 2022, **43**, 539-555.

8. T. Lu, F. Chen, *J. Comput. Chem.* 2012, **33**, 580-592.

9. W. Humphrey, A. Dalke, K. Schulten, *J. Mol. Graph. Model.* 1996, **14**, 33-38.